UNITED NATIONS EDUCATIONAL, SCIENTIFIC AND CULTURAL ORGANIZATION
INTERNATIONAL ATOMIC ENERGY AGENCY
INTERNATIONAL CENTRE FOR THEORETICAL PHYSICS
I.C.T.P., P.O. BOX 586, 34100 TRIESTE, ITALY, CABLE: CENTRATOM TRIESTE

SMR.1065 - 12

COLLEGE ON SOIL PHYSICS
14 - 30 APRIL 1998

"Applied time series analysis and geostatistical methods"

Donald R. NIELSEN
University of California, Davis
Department of Land, Air and Water Resources
Hydrologic Science
113 Veihmeyer Hall
CA 95616 Davis
U.S.A.

These are preliminary lecture notes, intended only for distribution to participants

REFERENCES ON REGIONALIZED VARIABLE ANALYSIS

Concept of a regionalized variable

Autocorrelation and crosscorrelation

Davis, J. C. 1973. Statistics and Data Analysis in Geology. John Wiley & Sons, Inc., New York

Nielsen et al., 1983. Analyzing field-measured soil-water properties. Agr. Water Mgt. 6:93-109

Buchter et al., 1990. Soil Spatial variability along transects. Soil. Tech. 4:297-314

Geostatistical methods

Variograms, covariograms, kriging and cokriging

Clark, I. 1979. Practical Geostatistics. Applied Science Pub. Ltd., London

David, M. 1977. Geostatistical Ore Reserve Estimation. Elsevier Scientific Publ. Co., New York

Journel, A.G., and Ch.J. Huijbregts. 1978. Mining Geostatistics. Acad. Press. New York

Vieira, et al., 1981. Spatial variability of field-measured infiltration rate. SSSAJ 45: 1040- 1048

Vauclin, et al., 1983. The use of cokriging with limited field soil observations. SSSAJ 47: 175- 184

Miller et al.,1988. Spatial variability of wheat yield and soil properties on complex hills. SSSAJ 52: 1133- 1141

Morkoc et al., 1987. Kriging with generalized covariances. SSSAJ 51: 1126-1131

Webster, R., and Oliver, M.A. 1990. Statistical Methods in Soil and Land Resource Survey. Oxford University Press, Oxford, UK.

Applied time series analysis

Spectral, cospectral analyses and coherency

Haan, C.T. 1977. Statistical Methods in Hydrology. Iowa State University Press, Ames, Iowa.

Chatfield, C. 1985. The Analysis of Time Series: An Introduction. Chatman and Hall, New York.

Shumway, R.H. 1988. Applied Statistical Time Series Analysis. Prentice-Hall, Englewood Cliffs, New Jersey

Bazza et al., 1988. Two-dimensional spectral analysis of soil surface temperature. Hilgardia 56: 1-28

Autoregressive functions

Morkoc et al., 1985. Statistical analysis of sorghum yield: A stochastic approach. SSSAJ 49:1342-1348

State space analysis

Field observations

Morkoc et al., 1985. Analysis of soil water content and temperature using state-space approach. SSSAJ 49(4):798-803

Wendroth et al., 1992. State-space approach to spatial variability of crop yield. SSSAJ 56: 801-807

Kachanoski and de Jong, 1988. Scale dependence and the temporal persistence of spatial patterns of soil water storage. Water Resour. Res. 24:85-91

Samra et al., 1993. Modeling competition of paired columns of Eucalyptus on interplanted grass. Agroforestry Sys. 21: 177-190

Combining deterministic equations with observations

Parlange et al.,1993. Determination of the field scale diffusivity function, soil water storage and evaporation, Water Resour. Res. 29: 1279-1286

Nearest neighbor analysis

Mulla et al., 1992. SSSAJ

Published in: Gregorich, E.G., and M.R. Carter (Editors). 1997. Soil Quality for Crop Production and Ecosystem Health. Elsevier Science Publishers B. V., Amsterdam.

Chapter 11

STATISTICAL APPROACHES TO THE ANALYSIS OF SOIL QUALITY DATA

O. WENDROTH, W.D. REYNOLDS, S.R. VIEIRA, K. REICHARDT and S. WIRTH

I. INTRODUCTION

Adequate management of the environment and agricultural resources requires assessment of soil quality. Inasmuch as we want to protect our global resources when managing agricultural systems, we have to achieve efficient use of inputs, such as fertilizers and pesticides, for crop production, as well as avoid pollution risks arising from over-application of agrochemicals. Therefore, spatial and temporal patterns of soil properties and soil quality attributes and indicators have to be known. Moreover, to integrate and regionalize information from specific points to larger scales, knowledge of the nature of spatial and temporal patterns of land surfaces is essential.

In this chapter, we discuss techniques that allow us to analyse field observations statistically. The concept behind these techniques differs from the classical way of conducting agronomic experiments. With new approaches, we no longer have to impose treatments that generally disregard a thorough understanding of the entire agricultural system (Peterson et al., 1993; Nielsen et al., 1994a). Instead, we can derive relevant information directly from on-site observations using tools that manipulate these observations to assess physical, chemical, and biological properties of entire fields (Nielsen et al., 1994b). These monitoring and analyzing methods help focus our attention on the underlying processes that account for the spatial and

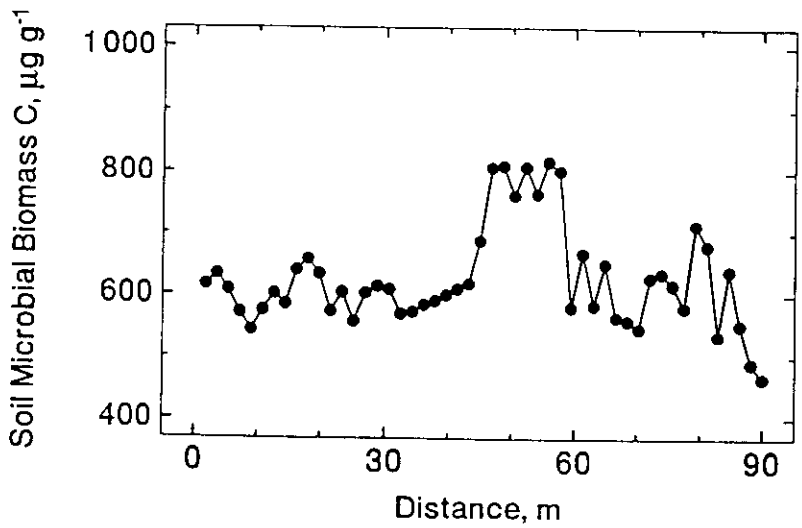

Fig. 11.1. Soil microbial biomass C along a transect sampled across a moraine catena in NE Germany.

$$r(h) = \frac{C(h)}{s^2} \tag{2}$$

where

$$s^2 = \frac{\sum_{i=1}^{N}(x_i - \bar{x})^2}{N-1} \tag{3}$$

In Figure 11.2a, the autocorrelation function for the biomass data is shown. We can obtain $r(h)$ by plotting the observations x_i against the observations x_{i+h}, and can then calculate the respective correlation coefficient $r(h)$ for this scatter diagram. With increasing lag distance, the number of pairs x_i versus x_{i+h} decreases, and therefore the reliability of $r(h)$ becomes small for widely separated observations (large h-values) unless N is very large.

Another tool reflecting the autocovariance versus lag relation is the semivariogram or simply variogram $\gamma(h)$, calculated according to the following:

$$\gamma(h) = \frac{1}{2N(h)}\sum_{i=1}^{N(h)}(x_i - x_{i+h})^2 \tag{4}$$

where $N(h)$ is the total number of sample pairs for the lag interval h. For the chosen sampling distance (h), half of the average squared difference between all pairs of observations separated by that distance is calculated. Unlike the autocorrelation function, the semivariogram is not based on the total sample variance but on variation between pairs of observations. Hence, it is not bound so strictly to stationarity assumptions as is the autocorrelation function. Stationarity means that

temporal variability patterns of soils and crops, rather than looking for a significan response to a set of imposed treatments that may not be practicable or even b related to optimal management practices for a particular field (Nielsen and Alemi 1989).

When farmers manage their fields, they intuitively pay attention to local soi variability within their fields—information that has often been suppressed ir agronomic studies. Now we have the opportunity to expand the intuitive thoughts o the farmer using analytical tools to provide better management alternatives designe specifically for each of his particular fields.

The objectives of this chapter are to illustrate basic principles, aspects, and requirements for spatial statistical analyses and to present some applications o selected geostatistical techniques (Isaaks and Srivastava, 1989) and time serie analysis (Shumway, 1988). This contribution should allow answers to the questions: For a given area such as a farmer's field or watershed, what are the patterns of soil properties, crop attributes, and yields that display spatial variability? How can these patterns be identified and understood? How can this identification and understanding be used to optimize profitability and agricultural and environmental sustainability?

II. APPROACHES

A. Autocovariance

Usually when a variable is sampled in the field, the mean and the variance are determined to reflect the sampled population, assuming that sampling occurred randomly and representatively (i.e., observations are independent of each other and, in general, are normally distributed).

The set of microbial biomass data sampled along a catena in a landscape ecology study shown in Figure 11.1 has a mean of 626.8 μg C g^{-1} and a variance of 6811.1 (μg C g^{-1})^2. Fifty samples were taken at 1.8-m intervals along a 90-m long transect. The following analysis shows additional information that a spatial analysis of a univariate data set can provide when sampling coordinates are considered, rather than ignoring them as is commonly done in most agronomic experiments. The autocovariance-lag distance function or simply the autocovariance function $C(h)$ is defined as

$$C(h) = \frac{1}{N}\sum_{i=1}^{N-h}(x_{i+h} - \bar{x})(x_i - \bar{x}) \tag{1}$$

where a set of N observations x_i at location i with mean $\bar{x}$ is considered (Salas et al., 1988). The distance between pairs of observations is h, the so-called lag. When C(h) is normalized (i.e., it is divided by the sample variance s^2) it is called the autocorrelation function $r(h)$, which is bounded between +1 and −1, and is determined by:

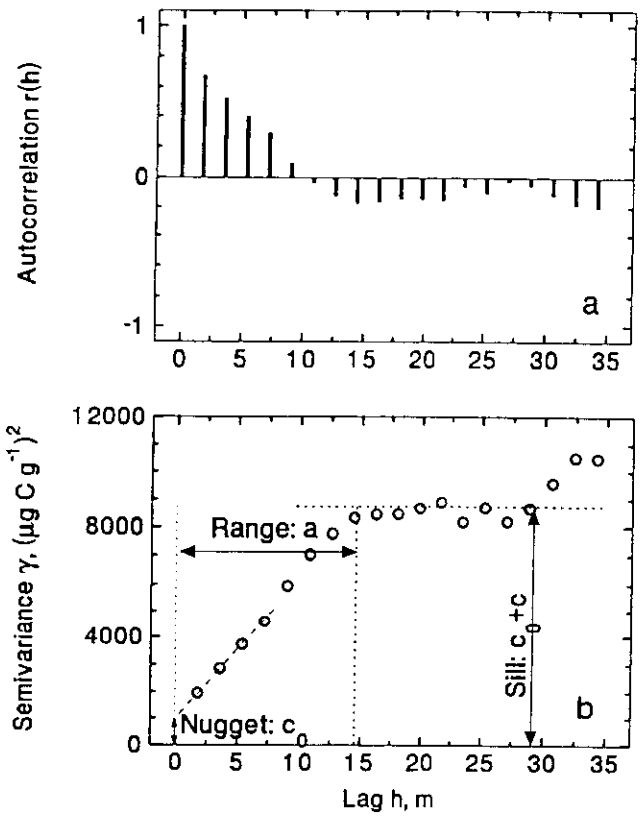

Fig. 11.2. Autocorrelation function (a), and semivariogram (b) for microbial biomass C data.

the mean and the variance of the data do not change appreciably within the samp region, which implies as a consequence that there are no overall trends or slope the data values with position. When stationarity exists the semivariogram (Fig. 11. is a mirror image of the autocorrelation function. The semivariogram can be used spatial interpolation purposes such as kriging (as shown in the example below land evaluation with respect to atrazine leaching).

Between 1.8 and 5.4 m (or between 1 and 3 lags) in Figure 11.1, the au correlation of biomass data decreases, and the semivariance increases stee (Fig. 11.2a,b). The zone of increasing semivariance is called the *range*. The ran which reflects the structured variability of observations, is 14.4 m or 8 lags in example (Fig. 11.2b). Hence, we can say that up to a distance of roughly 14 microbial biomass observations are correlated with each other. When the semiv ance does not change significantly with increasing lag distance, the plateau reache called the *sill*, reflecting the magnitude of random variation, which in our exampl around 8500 $(\mu g\ C\ g^{-1})^2$.

Although by definition $\gamma(h)$ equals 0 at $h = 0$ (i.e., the variability of the measu parameter is zero at zero distance from the location of measurement), the *nugget* is

effective value of $\gamma(h)$ at $h = 0$ extrapolated from values of $\gamma(h)$ for $h > 0$. The nugget reflects that fraction of the variance at the shortest sampling distance, that is attributed to measurement uncertainty (human error, measurement error, repeatability, etc.) and nested structures having ranges smaller than the sampling interval (Olea, 1991). In some cases, the magnitude of the nugget can be reduced by sampling at shorter h intervals. In the case of our example of biomass determination (Fig. 11.1), errors may arise from sample augering and preparation, calibration of the analyser (CO_2-detector), and measurement noise. The latter may be reduced by repeated measurement with the same sample if possible. In view of the small nugget variance in our example (approximately 1000 $(\mu g\ C\ g^{-1})^2$ and only 12% of the sample variance, Fig. 11.2b), the method for determining biomass is considered sufficiently reliable to allow satisfactory determination of its spatial structure of variation.

Up to a distance of 14.4 m, observations are spatially correlated (Fig. 11.2b) (i.e., having sampled at a location, the variance band is known for the expectation of a biomass value at a certain location by knowing neighboring values and their separation distances to that location). One may conclude from the biomass semivariogram that a structured variability could have been identified even if the separation distance between nearest samples were increased. On the other hand, if samples had been taken at distances greater than 15 m across this 90-m transect, they would have appeared to vary randomly in space. The effect would have been the same as if their coordinates had been neglected, namely no information would have been gained on representativity of the sampling for biomass or the spatial continuum of microbial biomass. In that case, no spatial interpolation would be possible. Moreover, if the investigator had sampled randomly and had by chance received only one instead of seven samples from the zone between 45 and 58 m (Fig. 11.1), where an underlying but unidentified process apparently caused high microbial biomass values, this sample value would probably have been interpreted as an outlier. But having gained seven samples close to each other yielding higher biomass values, and knowing their sampling locations, a degree of certainty is given to the investigator that a sampling or measuring error had not occurred, and that a process not yet determined caused higher values in that region of the transect. Next, a study could follow, investigating: 1) how the spatial pattern of this parameter looks at a different sampling time; and 2) whether the spatial pattern of microbial biomass is linked to other soil and agronomic properties.

B. Crosscovariance

Similar to the autocovariance, the spatial relation between different variables can be determined via the crosscovariance, namely the crosscorrelation function $r_{xy}(h)$ (CCF) and the cross-variogram $\Gamma(h)$. The crosscovariance as a function of lag distance describes the degree of linkage between two variables x and y, where one variable, the tail variable, lags behind the head variable by the lag distance h (see Davis, 1986; Shumway, 1988). The CCF is unsymmetric, whereas the crossvariogram (or covariogram) is symmetric. Because the $\Gamma(h)$ function is symmetric, it produces the same result regardless of whether the x variable is heading or tailing.

In the following example, the crosscorrelation function is calculated for almon (*Prunus amygdalus* Batsch) yields, measured for each of 62 trees within tw neighboring parallel transects in an almond orchard north of Sacramento, Calif. U.S.A. The two distributions of almond yield across each transect are simila (Fig. 11.3). The relation between the yields at the same position within the transect i reflected by the classical correlation coefficient, $r = 0.41$, which is also the result fo the CCF at lag $h = 0$ (Fig. 11.4). Although the relation between the two variable does not seem to be very tight, the crosscorrelation function (Fig. 11.4) indicates tha the observations are spatially related to each other over a distance of about 40 m. I this example the CCF becomes insignificant when $-0.2 < r_{xy}(h) < 0.2$. Hence although classical correlation indicates a low relation between the variables at th same position, spatial coincidence of both processes is identified when the local rang of spatial correlation is examined. Within a certain local range, one variable i certainly related to the other, and this relation can be used for estimating a variabl at an unsampled location by means of the spatial crosscovariance structure. I classical regression analysis, the estimation accuracy of a dependent variable depend on the uncertainty of the regression coefficients. Spatial regression techniques, on th other hand, account for correlation structures in the neighborhood of location i namely within $i \pm h$. Consequently, the estimation uncertainty of a dependen variable can often be reduced substantially by using spatial regression techniques a opposed to classical regression techniques.

Coregionalization procedures or models for spatial realizations of randon functions, such as kriging and cokriging, apply this concept. The governing krigin and cokriging equations can be found in Alemi et al. (1988) and Deutsch and Journe (1992). Kriging and cokriging are techniques that are used to estimate unsample

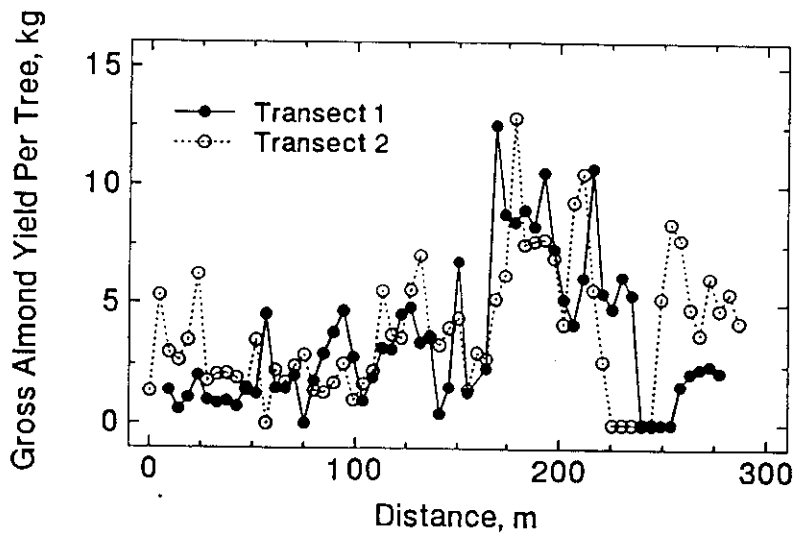

Fig. 11.3. Almond yields across two rows of almond trees in an orchard north of Sacramento Calif., U.S.A.

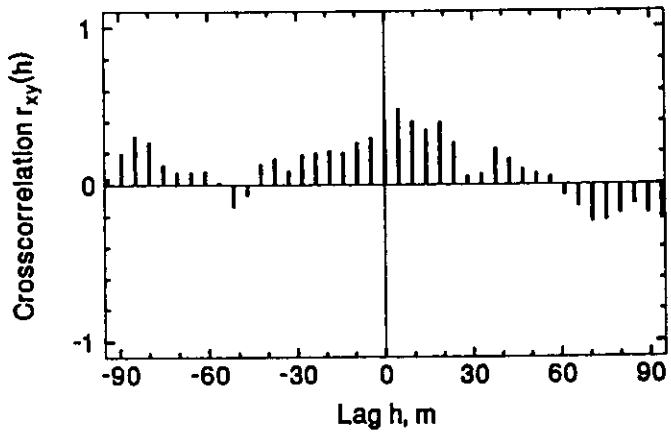

Fig. 11.4. Crosscorrelation function for almond trees in an orchard north of Sacramento, Calif., U.S.A.

data points from observed data. The estimation for an unsampled location is based on known values in the local neighborhood of the unsampled location. The amount that the known values contribute to the estimated value depends on the number of observed points in the vicinity of the location of interest. The weight of the contribution of the known values decreases with increasing distance away from the location of interest. Hence, the estimation is based on a linear combination of the neighborhood values. This estimation differs from that of classical regression analysis in which spatial relations between all locations are ignored, and only one equation reflects causal relations across the entire sampling domain. For kriging and cokriging, significant information obtained from the structure of variation (i.e., the variogram and crossvariogram, respectively) is incorporated as a measure of reliability of the estimation, namely the kriging and cokriging estimation variance (Alemi et al., 1988).

Cokriging can be applied for spatial interpolation, especially in situations in which sampling resources are limited but one needs to gain information about unsampled locations. This technique was recently examined as a multivariate geostatistical tool for yield response and N-pollution by Goovaerts and Chiang (1993). As an example of cokriging, we assume a scenario for the almond yield data across the two parallel transects where yield values are known for only 16 locations in transect 1 but for all locations in transect 2 (Fig. 11.5). In the cokriging procedure, the semivariogram of the variables of interest (Fig. 11.6a,b) and the crossvariogram (Fig. 11.6c) are the underlying information for the estimation variance in the interpolation procedure. The spherical model was chosen to fit the variogram data, as follows:

$$\gamma(h) = c_0 + c\left[1.5\frac{h}{a} - 0.5\left(\frac{h}{a}\right)^3\right], \text{ if } h \le a \qquad (5)$$

$$= c_0 + c \qquad , \text{ if } h \ge a \ .$$

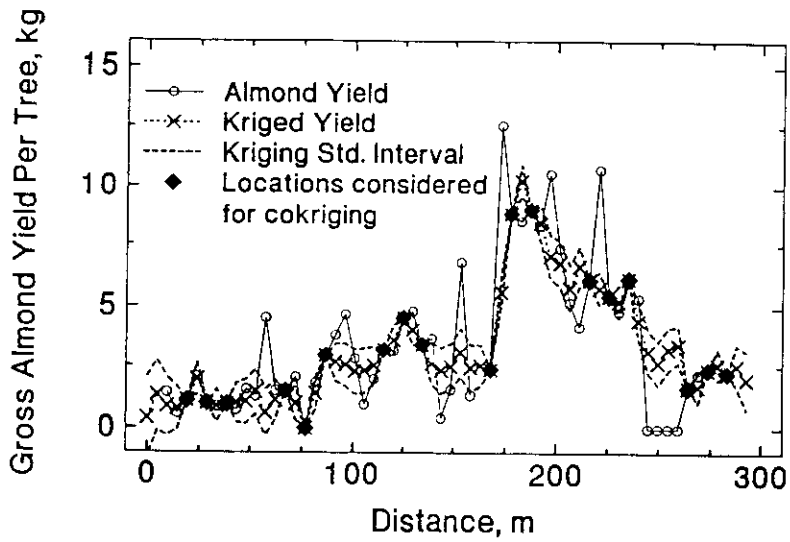

Fig. 11.5. Hypothetical scenario for cokriging of "unknown" almond yield values via spatial covariance.

In equation 5, c_0, c, a denote the nugget, sill, and the range (see Fig. 11.2), respectively. Because values of $\gamma(h)$ and $\Gamma(h)$ are most important at short distances, the observations in transect 1 were not spaced equally but in a nested structure (i.e., nests with short sampling distances were distributed over the entire length of the transect). The use of nested sampling allows a relatively small number of observations to adequately determine the semivariance at small sampling distances, and thereby reduce the nugget.

Like any other interpolator, cokriging smooths the spatial process of data and tends to fail especially at large fluctuations between neighbors. The standard estimation error intervals shown in Figure 11.5 become wider with increasing distance from the formerly observed point and decrease again when approaching the next observed point. Note that with classical regression the fiducial limits of estimation would be wider than for kriging, and also constant, regardless of the proximity of an observed point.

In this one-dimensional example (Fig. 11.5), the power of cokriging cannot be fully described. In two- or three-dimensional sampling designs, cokriging can be used for mapping purposes and can help to estimate patterns of variables based on the crosscovariance with "cheaper" variables. It can be used for coregionalization of different variables observed at the same location (or in a parallel array of locations, such as in our example of the two neighboring transects) and for prediction of spatial patterns at different times (e.g., relating crop yield patterns to those of soil water content; Bouten et al., 1992). Cokriging even allows anisotropic variation structure to be accounted for (i.e., when variograms have different slopes or shapes for different directions in space). At this point the more interested reader is referred to

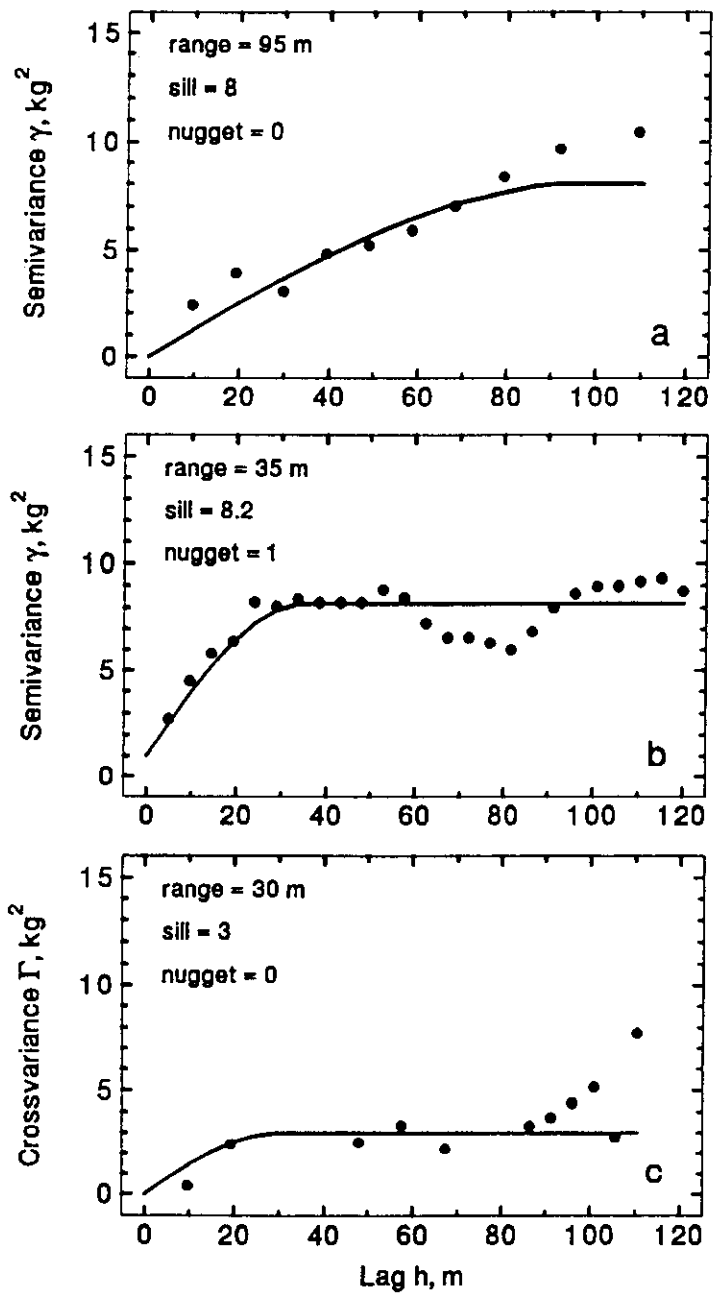

Fig. 11.6. Semivariograms for almond yields in row 1 (a), row 2 (b), and the crossvariogram (c). Parameters for spherical variogram model are given.

the literature (e.g., Alemi et al., 1988; Deutsch and Journel, 1992; Zhang et al., 1995 Halvorson et al., 1995).

Nevertheless, kriging and cokriging are dependent on the validity of the variograms and crossvariograms upon which they rely. Additionally, stationarity assumptions have to be met for kriging and cokriging applications, whereas other interpolation tools, such those presented in the following section, are not necessarily limited to stationarity conditions (Shumway, 1985).

C. *State-space analysis*

The state-space analysis (Shumway, 1988) demonstrated here is a special kind of autoregressive model. State-space analysis can be used, like kriging and cokriging for spatial interpolation but the philosophy behind this tool is different from that of kriging. In state-space analysis, a system's state (i.e., the state of a variable or of a set of variables) at location i, is considered with respect to the system's state at location $i - h$, where $h = 1,2,3, \ldots, n - 1$. These kinds of autoregressive tools are used for various kinds of forecasting based on the process of a series through the past to identify the coefficients linking system's states (the state coefficients) through space or time. Economical time series, remote controlled missiles, soil temperature and water content series (Morkoc et al., 1985a), crop yield and soil nitrogen status (Wendroth et al., 1992), and lake water storage (Assouline, 1993) are a few examples of data modeled with state-space approaches.

The basic equation, the so-called state equation, is as follows:

$$Z_i = \Phi Z_{i-1} + \omega_i \tag{6}$$

where Z_i is the state vector (i.e., a set of p variables at location i), Φ is a $p * p$ matrix of state coefficients indicating the measure of spatial regression, and ω_i is the uncorrelated zero mean model error. So far, this is the usual structure of common autoregressive models, where coefficients in the Φ matrix could be calculated via multiple regression. Here, Z_i is equivalent to the dependent and Z_{i-1} to the independent variable, respectively. Unlike common autoregressive models, however the "true" state of the variable or of the state vector in state-space models is considered embedded in the following observation equation:

$$Y_i = M_i Z_i + ny_i \tag{7}$$

where the observed vector Y_i is related to the true state vector Z_i via an observation matrix M_i and an uncorrelated mean zero observation error ny_i. In other words, what is measured does not have to be fully taken to be true, but can be considered as an "indirect measure" reflecting the "true" state of the variable plus noise (unidentified error). This error is associated with measurement uncertainty arising from reproducibility and validity of the calibration underlying the "indirect" observation. Note that almost every observation has to be considered as an indirect measure.

Moreover, unlike common autoregressive modeling, the state coefficient and covariance matrices are optimized via Kalman filtering (Kalman, 1960) within an iterative algorithm. Unlike multiple regression, the Kalman filter accounts for

measurement and model errors by not taking the measurements to be absolutely true but allowing for the variance of the state. In the state-space coefficient estimation, 1) the value at step i is predicted based on the state at $i-1$ and a given set of coefficients, 2) the prediction is compared to the measurement, and 3) the prediction is updated as far as the deviation between measurement and prediction requires, while accounting for both model and measurement errors. Steps 1 to 3 are repeated, while coefficients are optimized iteratively, until a convergence criterion is met. For further details, see Shumway (1988), Katul et al. (1993) and Nielsen et al. (1994a).

In the following example, observations of a field study from the International Atomic Energy Agency (IAEA) experimental field in Seibersdorf, Austria, described in Reichardt et al. (1987) were analyzed using a state-space approach (see also Wendroth et al., 1992). In two neighboring transects, a field experiment was established in order to estimate spatial variation of symbiotic nitrogen fixation of a legume crop, alfalfa (*Medicago sativa* L.). Soil and crops were sampled every 1.8 m across a 96-m long transect. The heterogeneous soil contained a considerable volume fraction of small stones that varied across the site (Fig. 11.7a). Knowing that soil nitrogen content affects both crop production and the rate of symbiotic nitrogen fixation, the soil nitrogen has to be considered on a volume basis as effective nitrogen *N*eff (Fig. 11.7b). Therefore, the volume of stones per unit soil volume was accounted for in the calculations. Based on the ^{15}N-isotope dilution method, nitrogen fixed under the alfalfa crop was determined (Fig. 11.7c). The crop yields of ryegrass (*Lolium* sp.) and alfalfa are shown in Figure 11.8.

In a scenario where we assume to know every *N*eff value, but only a cyclic sequence of three ryegrass yield observations followed by three unknown values the coincidence of *N*eff and ryegrass yield processes was determined. The result of the state-space estimation with the respective state equation is presented in Figure 11.9a. The underlying system of equations is as follows:

$$\begin{pmatrix} RY_i \\ N\text{eff}_i \end{pmatrix} = \begin{pmatrix} \phi_{11} & \phi_{12} \\ \phi_{21} & \phi_{22} \end{pmatrix} \begin{pmatrix} RY_{i-1} \\ N\text{eff}_{i-1} \end{pmatrix} + \begin{pmatrix} \omega_{RYi} \\ \omega_{N\text{eff}_i} \end{pmatrix} \tag{8}$$

i.e., the ryegrass yield at location i is determined as a function of ryegrass yield and *N*eff, both at location $i-1$, plus a model error ω. The estimated state coefficient matrix incorporates the spatial regression between neighboring locations as well as the effect due to measurement noise. For the alfalfa crop, both *N*eff and the nitrogen derived from the atmosphere (*N*dfa) caused variation of crop yield. In this case the equations take the form:

$$\begin{pmatrix} AY_i \\ N\text{eff}_i \\ N\text{dfa}_i \end{pmatrix} = \begin{pmatrix} \phi_{11} & \phi_{12} & \phi_{13} \\ \phi_{21} & \phi_{22} & \phi_{23} \\ \phi_{31} & \phi_{32} & \phi_{33} \end{pmatrix} \begin{pmatrix} AY_{i-1} \\ N\text{eff}_{i-1} \\ N\text{dfa}_{i-1} \end{pmatrix} + \begin{pmatrix} \omega_{AYi} \\ \omega_{N\text{eff}_i} \\ \omega_{N\text{dfa}_i} \end{pmatrix}. \tag{9}$$

For alfalfa, yield values and *N*dfa values were assumed to be known only for those locations with closed symbols (Fig. 11.9b).

The model results show that for those locations where ryegrass and alfalfa yield values were ignored (Fig. 11.9b; open symbols), the 95% fiducial limits of estimation increased with distance from the observed location. For both crops, however, the

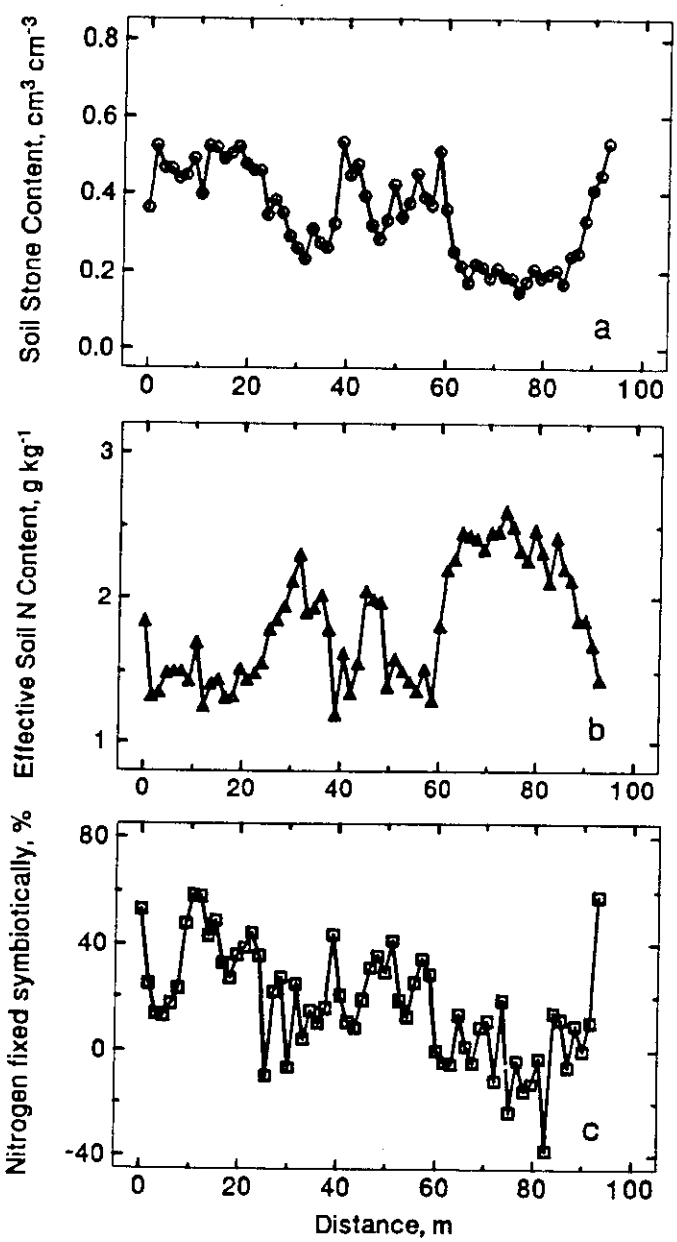

Fig. 11.7. Stone content (a), effective soil nitrogen content *N*eff (b), and the fraction of nitroge fixed from symbiotic N assimilation *N*dfa (c) in an experimental field in Seibersdorf, Austria.

estimation accuracy of the state-space model was generally sufficient, and the model tended to fail only when large fluctuations occurred between neighboring points This example also shows that, although many other parameters might hav

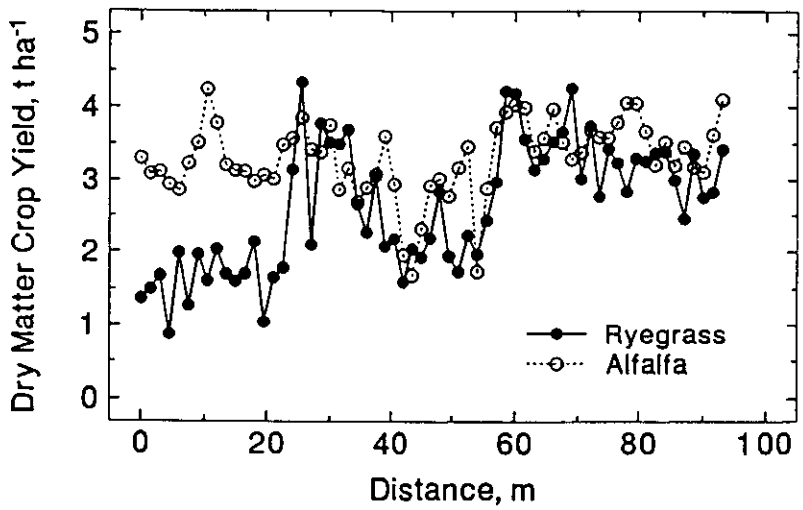

Fig. 11.8. Ryegrass and alfalfa dry matter yield across the transect in an experimental field in Seibersdorf, Austria.

influenced the spatial process of crop yield and symbiotic nitrogen fixation (e.g., soil texture, air-filled porosity, soil temperature, soil water status, oxygen deficiency in the rhizosphere, pH value, organic matter content, micronutrients essential for symbiotically fixing enzymes, etc.), they do not necessarily have to be sampled. The importance of their unsampled contributions in causing deterministic influences on crop growth and yields is integrated into the model error (Nielsen et al., 1994b). Whenever state-space model errors are small, partial information derived quickly from on-site monitored observations can improve our understanding of the field situation and thereby provide a basis for better management decisions. In such situations the quickly observable variables reflect the main underlying process in fields. On the other hand, whenever state-space model errors are unacceptably large, additional or different soil or environmental parameters must be measured or derived either through existing knowledge or deterministic research.

D. Spectral analysis

Knowledge of the spatial pattern of soil properties is necessary for achieving higher efficiency of input for crop production. Such knowledge can also indicate the impact of previous agricultural management practices. Most agricultural field operations occur with a regular pattern. For example, a tractor goes back and forth across the field with an implement in parallel paths at regular intervals. Also, plants are grown with a regular pattern in order to decrease inter-crop competition and to increase water, light, and nutrient use efficiency. Moreover, considering the time domain, many field soils are subject to a certain crop rotation system, repeating in cycles of several years. Hence, periodic patterns develop spatially, temporally, or in

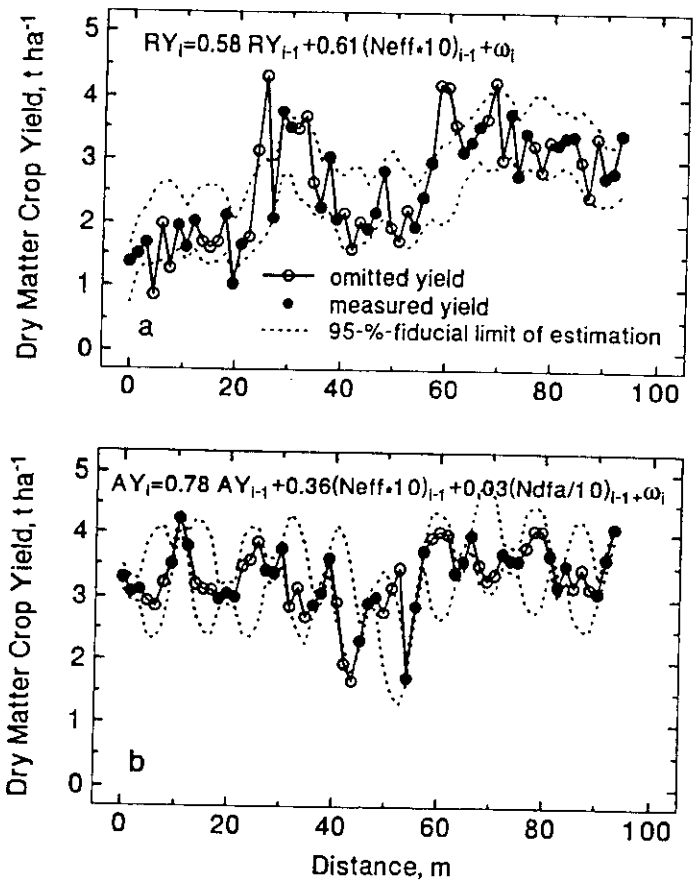

Fig. 11.9. State-space estimation of ryegrass yield (a) and alfalfa yield (b) across the transect in an experimental field in Seibersdorf, Austria.

both domains. Nielsen et al. (1983) showed how variation of soil moisture can be separated into cyclic components, corresponding to management operations. Bazza et al. (1988) applied a procedure known as spectral analysis to soil temperature data to show that patterns in these data coincided with the sinusoidal application pattern of irrigation water with different salt content. Using standard correlation methods, Kachanoski et al. (1985a) found that microtopography and A-horizon parameters were not related. However, when they considered the sampling coordinates of the parameters, and applied cospectral and spectral analysis techniques, it was found that spatio-periodical relations did indeed exist.

A series of observations can manifest various periodic patterns with different amplitudes and different lengths of cycles. The length of a periodic cycle is designated by the wave length (λ) or period, which is the inverse of the frequency (Davis, 1986). As a hypothetical example, three series with wave lengths of 4, 15, and 45 (i.e., one cycle every 4, 15, and 45 length units), respectively, and different amplitudes are drawn in

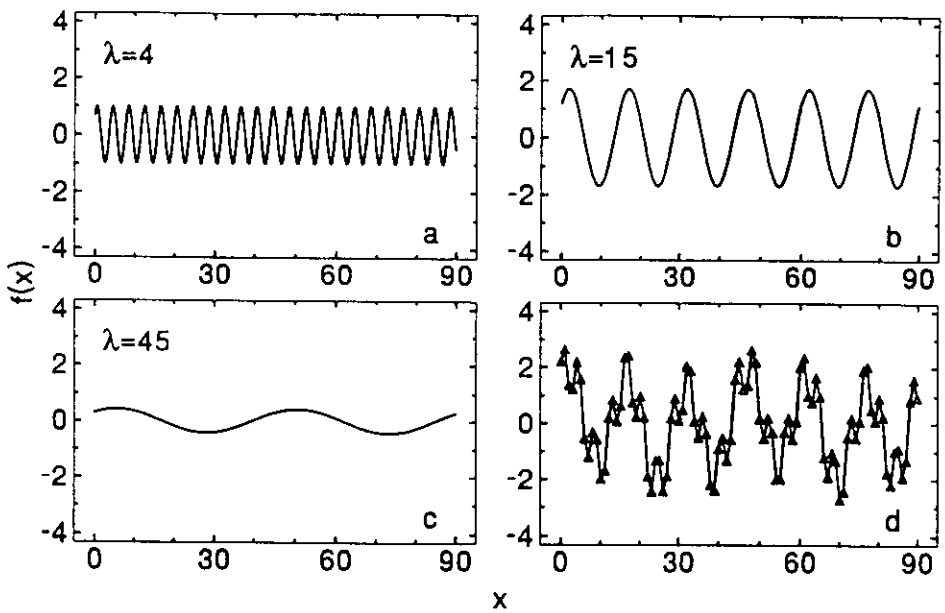

Fig. 11.10. Hypothetical sinusoidal series of different period and amplitude (a, b, c), and the integrated series, "sampled" at 91 locations (d).

Figure 11.10a,b,c. In the literature, short-range variation is often attributed to agricultural management practices (Trangmar et al., 1985, Kachanoski et al., 1985b, Moulin et al., 1994), whereas long-range variation reflects geologic components. When the three patterns are superimposed and sampled at 91 positions with observations separated by one length unit, one gets the confounded pattern in Figure 11.10d.

The power spectrum $f(\lambda)$ of the process x_i as a function of wave length λ is obtained via Fourier transformation by the following:

$$f(\lambda) = \sum_{-\infty}^{\infty} C(h) \exp[-2\pi i \lambda h] \tag{10}$$

where $i^2 = -1$

Spectral analysis filters the periodic variance components, shown in Figure 11.11 for the hypothetical example. One can find the three peaks in the power spectrum at the corresponding frequencies of 1/4, 1/15, and 1/45 (length units)$^{-1}$, respectively. Having determined a cyclic behavior of a series, one may use the knowledge about the period to make forecasts (e.g., forecasting the weather or river levels is a common practice in the meteorological and hydrological sciences; Kite, 1989).

The example here is yields across the two neighboring transects of the almond orchard considered above (Fig. 11.3), which are later used for cokriging (Fig. 11.5). Sprinklers were located after every third tree in the orchard, and the farmer was interested in whether this sprinkler arrangement affected tree growth. If this was so, the effect should have accumulated over the years and be manifested in a periodic

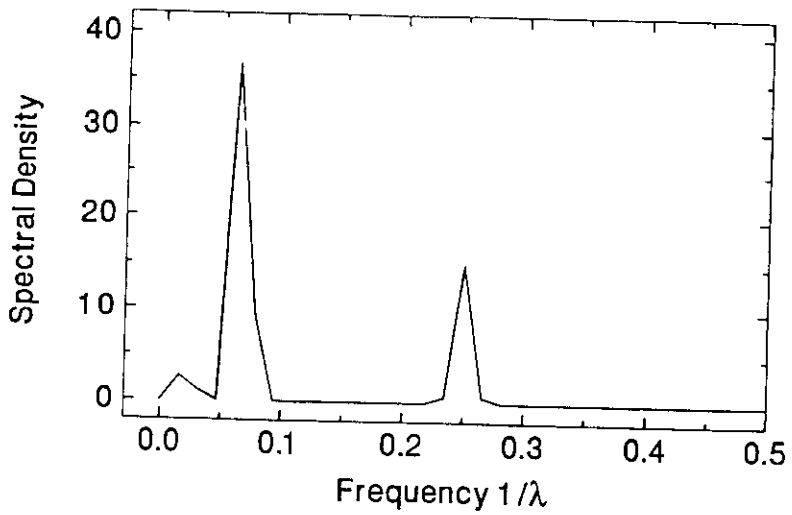

Fig. 11.11. Power spectrum for the hypothetical data set in Fig.11.10d.

variation of some easily obtainable tree growth parameters. For this purpose, trun circumference of trees within a transect (Fig. 11.12) measured at 50 cm above the so surface was analysed after the original data had been detrended. A peak appears at frequency close to 0.33 in the power spectrum (Fig. 11.13) (corresponding to a perio of every third tree). That this peak occurs at the same frequency as that of spati sprinkler distribution indicates that irrigation design does effect tree growth. Th increase of the power at $1/\lambda = 0.5$ (length units)$^{-1}$ reflects the fluctuation from or tree to the next and is perhaps due to inter-plant competition.

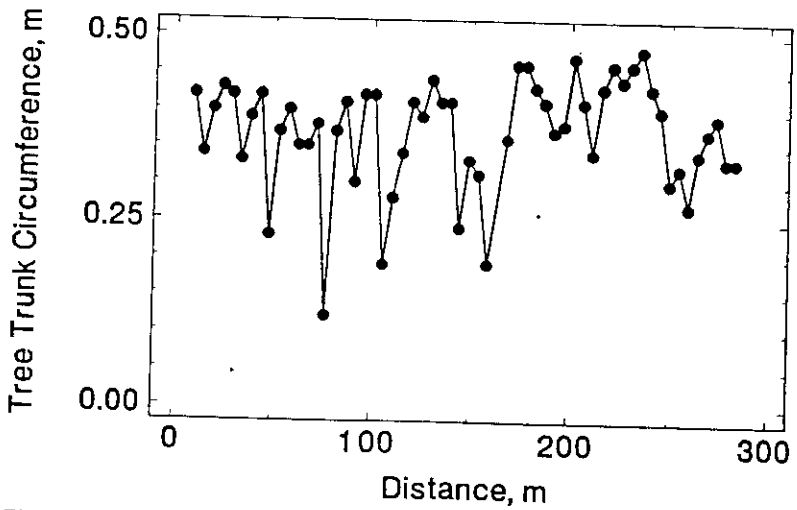

Fig. 11.12. Trunk circumference of almond trees in a transect north of Sacramento, Calif., U.S.A

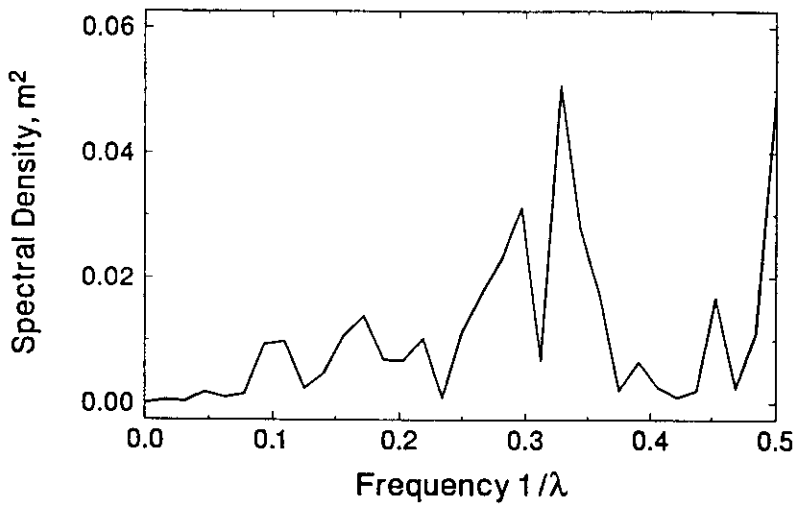

Fig. 11.13. Power spectrum of detrended almond tree trunk circumference in a transect (from Fig. 11.12) north of Sacramento, Calif., U.S.A.

When conducting spectral analysis, one must use samples at regular intervals in space or time. Moreover, the sample frequency should be higher than the expected frequency of the process or pattern being examined. This may cause laborious sampling, but sampling can be undertaken instantaneously and directly without designing any experiment or invoking any treatment in the field. Moreover, simple variables can be examined on-site (e.g., tree trunk circumference) to give direct information about the specific site to the farmer. In the almond orchard example, it would have been a monumental effort to design a field experiment in which the effects of sprinkler position had to be investigated in a randomized block experiment and the assumptions for classical statistics had to be obeyed (i.e., that observations had to be independent of each other). Had a randomized block experiment been conducted, still no information for the farmer's site would have been obtained.

One can also use spectral analysis to determine whether the frequency-dependent variations of two series of observations coincide (i.e., whether they are coherent). For example, the squared coherence function $\kappa(\lambda)$, as a measure of frequency dependent correlation, is determined for the two series of almond yields in parallel transects (Fig 11.3) according to:

$$\kappa_{yx}(\lambda) = \frac{[f_{yx}(\lambda)]^2}{f_x(\lambda) f_y(\lambda)} \tag{11}$$

where $f_{yx}(\lambda)$ is the cross spectrum (Shumway, 1988). The squared coherence for frequency-dependent analysis of variance is analogous to the coefficient of determination in classical regression and has values between 0 and 1. It indicates at which wavelengths two series proceed coherently or coincidently. Therefore, the squared coherence is 1 at all frequencies if one series x_t is an exact linear filter of

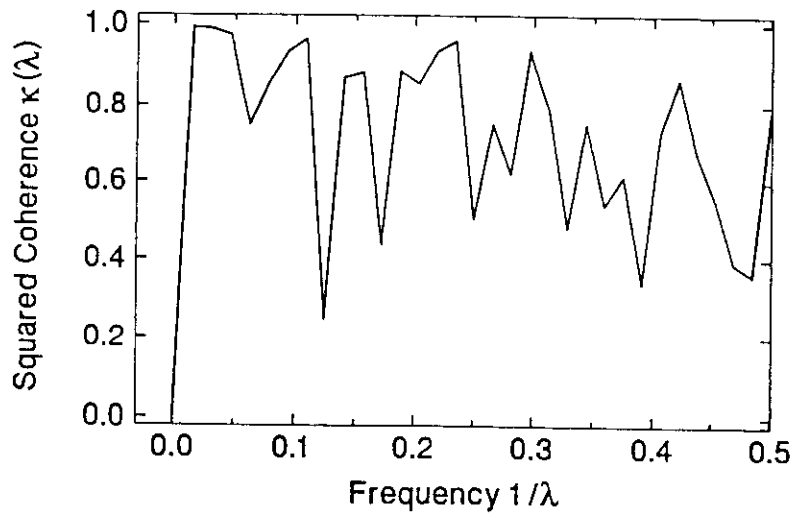

Fig. 11.14. Squared coherence of almond yields in two parallel rows (see Fig. 11.3) in an orchard north of Sacramento, Calif., U.S.A.

another series y_t. The spectrum of squared coherence of the almond yields in the parallel transects (Fig. 11.14) shows a strong coherence for several short wavelengths and especially for long wavelengths, and may indicate similarities in the periodic variation of some underlying soil properties and growing conditions in both transects.

E. Analyzing spatially variable field observations with physically based equations

Thus far in this chapter, we have advocated the use of spatial statistics in addition to the currently used classical methods. In both cases the statistical analyses examine variance and covariance functions derived from observations and measurements without explicitly invoking a physically based equation. The various kinds of observations selected were expected to be correlated based upon a conceptual knowledge of the processes occurring in the field. If correlations were not found, other kinds of observations would have to be selected by trial and error. Here we introduce the idea of using a physically based equation in combination with a set of observations expected to be correlated in space (or time).

A nonlinear partial differential equation describing a physically based process occurring at the soil surface can be derived and transformed into a state-space formulation. The process may be physical, chemical, or biological in nature (e.g., infiltration, nitrification, the leaching of soil solutes in the presence of plant root extraction, etc.). Such state-space models simultaneously examine a theoretical equation, its empirical parameters, and the observations that embrace the uncertainties of soil heterogeneity and instrument calibration. The usefulness of this approach lies in the opportunity to be guided by an equation expressing a process

that occurs at the soil surface and to simultaneously analyze the uncertainty in both the equation and our field measurements. Examples of progress recently achieved to improve our assessment of soil quality using state-space approaches include the examination of evaporation (Parlange et al., 1993) and infiltration and redistribution of soil water (Katul et al., 1993; Wendroth et al., 1993).

A desirable feature of the state-space methodology is the inclusion of an observation error that can be treated as a known, measured quantity or, alternatively, as an unknown for which a solution is found in the numerical scheme. The magnitude of a known observation error allows a reconsideration of the state variable in the equation or an improvement in instrumentation or calibration. On the other hand, by treating the observation error as an unknown, its behavior in space and time can be related to spatial and temporal correlation lengths that may manifest themselves within the domain of the field being studied.

As an example for applying physically based equations in the state-space analysis, the soil water transport equation is employed in order to determine the hydraulic conductivity function of a soil layer from time series field observations of soil water content $\theta(t)$ and hydraulic head difference across depth (i.e., the hydraulic gradient, $(\mathrm{d}H\mathrm{d}z^{-1})(t)$) (Fig. 11.15). These series were determined during water redistribution of an internal drainage experiment that was undertaken at the Campbell Tract experimental field of the University of California, Davis. Details of the underlying experiment are given in Katul et al. (1993) and Wendroth et al. (1993).

A soil layer between the upper depth z_i and the lower depth z_{i+1} is considered, for which we want to estimate the hydraulic conductivity–soil water content relationship $K(\theta)$. The soil water storage in this layer is W defined as follows:

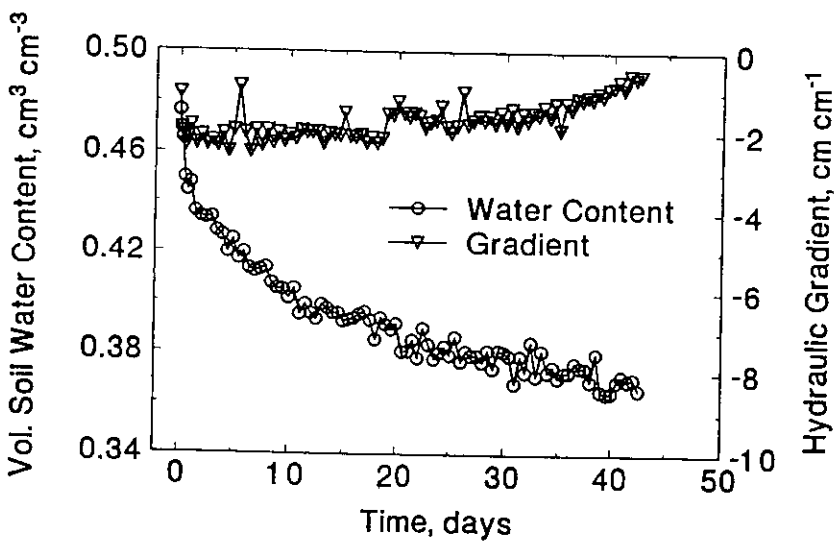

Fig. 11.15. Soil water content and hydraulic gradient time series in the surface soil layer during 43 days of an internal drainage experiment in Davis, Calif., U.S.A.

$$W = \int_{z_i}^{z_{i+1}} \theta \, dz \tag{12}$$

In the experiment, the plot was covered with a plastic sheet to prevent any soil wate flux at the upper boundary (q_i), hence the upper boundary condition is zero flux. Th water storage change in time of the upper soil layer that we are interested in has to b attributed to drainage flux (q_{i+1}) at depth z_{i+1}. The water storage change in time i then:

$$\frac{\partial W}{\partial t} = -q_{i+1} + q_i \ . \tag{13}$$

The force that is driving the flux q_{i+1} (i.e., the hydraulic head H difference acros depth) is measured at the center between z_i and z_{i+1} and below z_{i+1}. Using Darcy' law, Equation 13 can be written as follows:

$$\frac{\partial W}{\partial t} = -K(\theta)\frac{dH}{dz} + q_i \tag{14}$$

Note, that $K(\theta)$ is the function in which we are interested. This function reflect highly relevant soil pore system properties influenced by soil type, land use an management. It is often used in equations for irrigation control, water budg modelling, forecasts, etc.. The following simple two-parameter exponential functio is employed:

$$K(\theta) = A\exp(BW) \ . \tag{15}$$

Combining Equations 14 and 15 yields

$$\frac{\partial W}{\partial t} = -A\exp(BW)\frac{dH}{dz} + q_i \ . \tag{16}$$

In order to formulate a state-space equation, soil water storage in the dept compartment is considered as the state variable $X(t)$. Moreover, model errors $\omega($ are included and can be addressed to misleading assumptions underlying Equatior 14 and 15. The state-space equation is then:

$$\frac{dX(t)}{dt} = -A\exp(BX(t))\frac{dH}{dz}(t) + q_i(t) + \omega(t) \ . \tag{17}$$

Inasmuch as the true state of soil water storage in the soil compartment cannot b determined but is estimated indirectly with a neutron probe, an observation equatio has to be defined as follows:

$$Z(t_k) = X(t_k) + ny(t_k), \quad k = 0, 1, 2, 3, \ldots \tag{18}$$

The noise term $ny(t_k)$ accounts for instrumental calibration and measurement erro of the neutron probe.

In the state-space analysis, an expectation for Equation 17 and the variance bein the squared difference between state and state expectation are calculated (see Kati et al., 1993). The propagation of the state and its variance need to be solve simultaneously. Initial estimates of $K(\theta)$ model parameters A and B, and of som

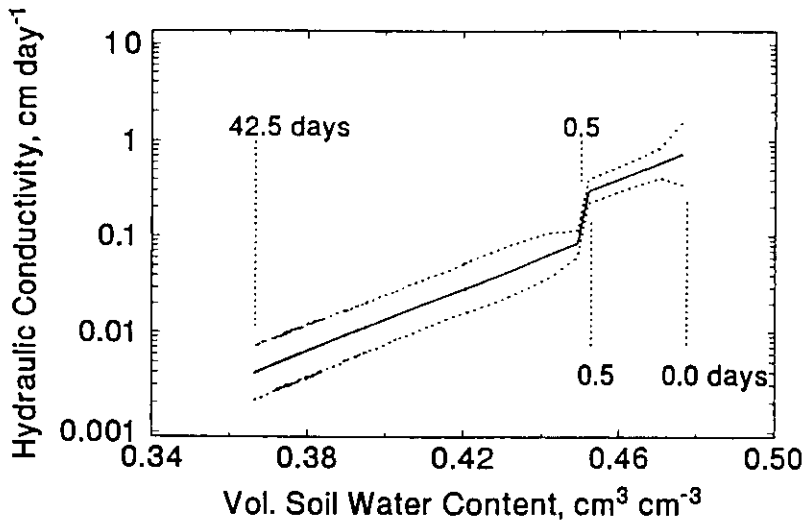

Fig. 11.16. Hydraulic conductivity as a function of soil water content determined from the internal water drainage in the surface soil layer (from Fig. 11.15) in Davis, Calif., U.S.A.

initial conditions are given. These are iteratively optimized via prediction, comparison between the prediction and the observation, and updating of each time step with respect to the variance. At this point the more interested reader is referred to Gelb (1974), Katul et al. (1993) and Wendroth et al. (1993).

The resulting $K(\theta)$ relation is shown in Figure 11.16. In order to achieve an appropriate prediction of $\theta(t)$, the water content time series was divided into two domains, one observed during the first 12 hours of the experiment, the other afterwards, probably manifesting transport phenomena and properties at different pore domains. In the range of high water contents, mainly macropores contribute to water transport, whereas $K(\theta)$ apparently follows a different relation in the drier range. For further details, see Wendroth et al. (1993).

This application of state-space analysis and Kalman filtering seems to be similar to an inverse estimation procedure, such as that of Kool and Parker (1987), where a transport model equation repeatedly runs in combination with a nonlinear optimization routine until a convergence criterion for a set of empirical parameters is met (i.e., the objective function is optimized). Nevertheless, there exist distinct differences between the inverse procedure and the state-space analysis. These differences are the same as those mentioned earlier when comparing estimation of autoregression coefficients in a classical regression analysis versus state-coefficient estimation in the Kalman filtering procedure. Neither the classical regression nor the inverse nonlinear optimization of an empirical relation in combination with a physically based equation account for measurement and model error, nor do they imply an updating within the range of possible variance resulting from measurement and model uncertainties. Instead of taking advantage of observations during prediction of a series wherever they become available, as it is done via updating in

the Kalman filter, inverse procedures compare observations and estimations only within the objective function at the end of an iteration step. Unlike Kalman filtering they do not incorporate any quantity of model error nor yield any measurement error, respectively.

F. Combining water and solute transport models with geographic information systems

Similar to the state-space approach presented above, the following example also takes advantage of physically based equations. Reynolds et al. (1994, 1995) used a mechanistic water and solute transport model in combination with georeferenced soil, weather and crop management data to estimate the potential for leaching of the herbicide, atrazine, into the ground water under an entire watershed. The model which was a modified form of the modelling package LEACHM (Hutson and Wagenet, 1989) integrated the major processes that occur in the soil profile including soil horizonation; saturated, unsaturated, steady and transient water flow crop management, growth, and transpiration; solute sorption, degradation, advection, and dispersion; precipitation and evaporation; soil heat flow; and water table elevation. Soil survey information was used to obtain the required model input data on soil properties. Archived weather data records were used to derive the necessary model input for weather. Crop management practices for a corn (*Zea mays* L.) crop were assumed, with planting, harvesting, and atrazine application dates being determined by both soil properties and weather. All input data were georeferenced to the centroids of 119 soil landscape polygons that encompassed the watershed of interest. The model was run at each of the 119 landscape polygon centroids for a period of 10 consecutive model years; and model predictions of 1) annual atrazine loading at the 90-cm (average tile drain) depth, and 2) elapsed time for atrazine to reach the 3-ppb concentration (U.S. EPA drinking water limit) at the 90-cm depth were collected in space and time. Kriging was then used to convert the 119 irregularly spaced and highly variable point values of soil properties, weather data, and predicted atrazine loadings and concentrations into 1657 interpolated values extending throughout the watershed on a regular 2 km by 2 km grid. The kriged interpolations accomplished the required extension from a point basis (polygon centroids) to an areal basis (watershed), while still retaining the spatial variability characteristics of the original data. The kriged data also provided the spatial detail necessary to allow a Geographic Information System (GIS) to effectively produce and overlay maps of atrazine loading and concentration, soil properties, and weather data.

The predicted atrazine loadings to the 90-cm depth were found to be highly variable and complexly distributed throughout the watershed (Fig. 11.17). Comparison of this loading map to soil texture and summer precipitation maps for the watershed (texture and precipitation maps not shown) revealed that the lowest atrazine loadings occurred where soils were clayey and summer precipitation was low, whereas intermediate to high loadings occurred on sandy to loamy soils where summer precipitation was moderate to high. Correlation analysis showed further that atrazine loading was significantly correlated with many soil and weather

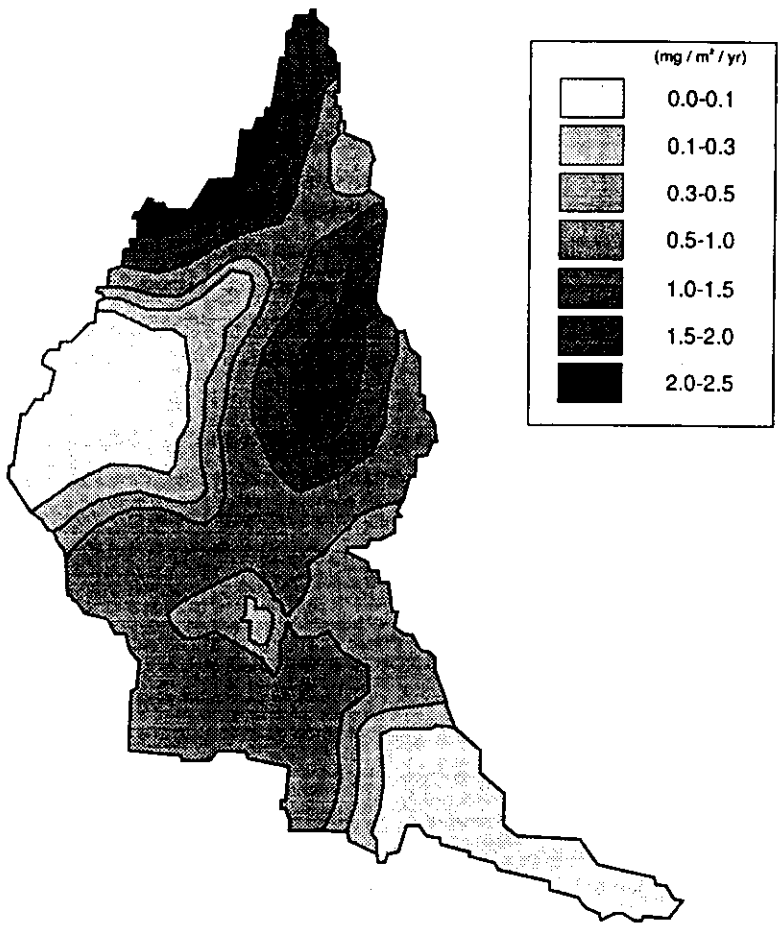

Fig. 11.17. Annual atrazine loadings (mg atrazine m^{-2} yr^{-1}) at the 90-cm depth for the Grand River watershed, Ontario, Canada.

parameters, but the magnitudes of these correlations were generally low. This suggests that atrazine loading in the watershed was determined by complex interactions among several soil, weather, crop management, and solute transport factors, rather than by one or two dominant factors.

The concentrations of atrazine in the soil water at the 90-cm depth were predicted to be generally low throughout the watershed (Fig. 11.18). The 3 ppb U.S. EPA drinking water guideline for atrazine was exceeded, however, on or before the tenth simulation year in about 27% of the watershed area (Fig. 11.18). The areas where this occurred also have predicted annual atrazine loadings that fall within the top half of the loading range (i.e., 0.5–2.5 mg atrazine m^{-2} $year^{-1}$, Fig. 11.17), which may consequently suggest that Figure 11.18 demarks regions of potentially significant low-level non-point source contamination of groundwater by downward migration

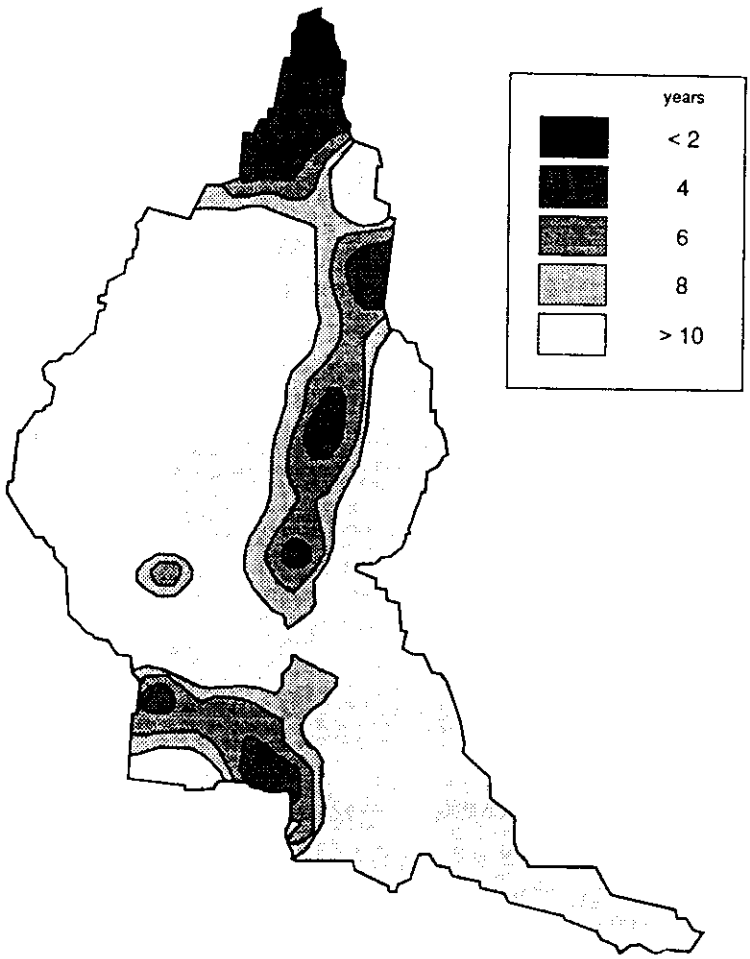

Fig. 11.18. Predicted time for atrazine to reach the 3-ppb concentration at the 90-cm soil depth i the Grand River watershed, Ontario, Canada.

of atrazine through the soil profile. Further more detailed investigations ma therefore be warranted in the areas where atrazine concentrations are predicted to b above the U.S. EPA limit.

Although combined simulation model–geostatistics–GIS analyses are still in th preliminary stages of development, it is clear from the above example that suc analyses are potentially very powerful and useful. These analyses could potentiall be used to determine the importance and spatial-temporal distributions of a proces (e.g., pesticide leaching); to determine the major soil, land use, and environmenta factors controlling the process; to estimate the potential environmental impact c changes in land use and land management; and to help establish land use and lan management practices that are both optimal and environmentally sustainable.

III. CONCLUSIONS

As a compendium of approaches described in this chapter, Table 11.1 gives an overview of the main statistical approaches currently being used in soil science. As Table 11.1 represents only a small proportion of what is possible, many new statistical approaches will undoubtedly be applied in the future.

TABLE 11.1

Compendium of approaches for assessing soil quality based on spatial and temporal statistics

Tool	Purpose	References
Autocorrelation Function	Plot of the correlation of a variable with itself across a distance h (lag); reflects the spatial or temporal continuum; assumed to be zero in ANOVA, regardless of the distance between observations	Shumway (1988), Morkoc et al. (1985b), Isaaks and Srivastava (1989)
Semivariogram (Variogram)	Plot of half of the average squared difference between observations separated by a distance h; like a mirror image of the autocorrelation function; reflects the range over which observations are correlated; parameterized by various models with nugget, range, and sill for interpolation (applied in kriging, and cokriging)	Vieira et al. (1981), Trangmar et al. (1985), Davis (1986), Nielsen and Alemi (1989),
Kriging	Spatial interpolation; estimation of values for unsampled locations, based on values at neighboring locations and the spatial (or temporal) variability structure (manifested by the variogram); estimation of confidence bands for interpolated value; jack-knifing is a special kind of kriging for validation of a variogram model	Vieira et al. (1981), Warrick et al. (1986), Alemi et al. (1988),
Crosscorrelation Function	Plot of the correlation between two variables as a function of their separation distance (lag); reflects the distance over which one variable is correlated with the other; length of crosscorrelation reflects the distance over which it is valid to correlate one variable with another	Nielsen et al. (1983), Davis (1986), Shumway (1988)
Crossvariogram (Covariogram)	Reflects the range over which observations of one variable are related to another; parameterized in the same manner as a variogram; used input for (applied in cokriging)	Alemi et al. (1988), Kachanoski and De Jong (1988), Zhang et al. (1995)

Table 11.1 (continued)

Tool	Purpose	References
Cokriging	Multivariate interpolation of values at unsampled locations; often applied to estimate expensive variables (sampled at low density) based on the spatial (or temporal) pattern of a cheap variable (sampled at high density); estimation of confidence bands based on the variograms and the crossvariogram	Alemi et al. (1988), Deutsch and Journel (1 Smith et al. (1993), Zhang et al. (1995), Halvorson et al. (1995)
State-Space Analysis	Special autoregressive approach; reflects the relation between the state of one or several variables to the state at previous locations (or times); spatial interpolation of unsampled locations; unlike kriging, not limited to stationarity assumptions; accounts for measurement and model uncertainty; incorporates as much deterministic input as necessary and integrates un sampled information on the basis of relations between neighboring observations.	Morkoc et al. (1985a), Nielsen and Alemi (198 Wendroth et al. (1992), Parlange et al. (1993), Katul et al. (1993), Wendroth et al. (1993), Nielsen et al. (1994a)
Power Spectrum	Decomposing the variation or fluctuation of a series of observations, which is sampled at regular intervals, into periodical components; reflects amplitude and frequency regardless of phase shift; often used to predict hydrological time series; detects effects due to the regular pattern of agricultural operations	Nielsen et al. (1983), Davis (1986), Kachanoski et al. (198 Bazza et al. (1988), Shumway (1988)
Coherency	Reflects at which wave lengths or periodicities two series fluctuate coincidently, regardless of any phase shift between the two series; equals 1, if a series is linear filter of another series; analogue to the coefficient of determination	Nielsen et al. (1983), Bazza et al. (1988), Shumway (1988)

The above examples were intended to give some insight into opportunities assessing soil quality using spatial and temporal statistical approaches. Overa number of statistical tools are available for sampling and analysing spatial temporal processes in ecosystems and agricultural landscapes. Nevertheless, t are no unique answers to questions regarding appropriate sampling schemes sampling scales. Most investigators commonly use sampling schemes consistent deterministic concepts applied to small areas or volumes at a specific loca

Although mindful of the much larger dimensions of the domain, plot, field, or agricultural landscape across which the observation or measurement will be interpolated or extrapolated, most investigators think of only one scale—that which is most convenient for the parameterization of the deterministic soil or crop property at a specific location. From the information presented in this chapter, it is obvious that the investigator needs to consider two different scales of observation. The first is the small scale associated with the minimum distance between pairs of observations below which interpolation of values can be neglected. The second is the large scale associated with the maximum distance between pairs of observations above which extrapolation of values can also be neglected. As an example for the consideration of crop production in a farmer's field, the minimum distance might be the distance between individual plants while the largest distance would be the length of the entire field managed in the same manner. Hence, after choosing the kinds of measurements or parameters to be observed, the researcher must decide upon the minimum distance to take observations and an adequate sampling method to achieve a spatial (or temporal) continuum within the entire, larger domain.

Vieira et al. (1981) recommended a spatial density of samples just necessary to detect the spatial continuum and to take additional samples separated by shorter distances in order to improve the estimation of a semivariogram close to the origin for decreasing the estimation variance with spatial interpolation. This improvement can be achieved with so-called nested sampling. One still has to keep in mind that spatial structure may vary between different variables, such as crop yield and soil parameters (Warrick and Gardner, 1983). Moreover, spatial structure changes with time, especially for agronomically relevant variables such as NO_3-N content (Cahn et al., 1994). On the other hand, Or and Hanks (1992) found similar spatial structures for soil water, crop height, crop yield variability, and irrigation water.

The approaches presented here can be easily expanded to different scenarios of on-site and landscape sampling in the space and time domain. They do not give answers to every question, and sometimes they fail. On the other hand, applying spatial statistics on data from field experiments which were originally designed for ANOVA is usually inappropriate or inadequate. Agricultural designs for ANOVA require that observations between treatments be spatially and temporally independent and if observations are not found to be independent in the ANOVA design, there are usually too few observations to make reliable conclusions using spatially dependent concepts.

If spatially variable concepts and appropriate statistical analyses are initially considered in the design of assessing soil quality, the kinds of questions and breadth of answers achievable are more comprehensive and much more flexible than those limited to the classical ANOVA traditionally used in soil and agronomic sciences.

Imposing treatments and looking for an average behavior of a certain kind of treatment on a soil assumed to be homogeneous on the average can be avoided with spatial statistics. Instead, spatial statistics allows direct sampling and analysis of field information for the benefit of resources management. Moreover, with noise or variance components (model and error) being accounted for within prescribed fiducial limits, the results are often much more relevant than average values.

Around the world, the request upon scientists focuses increasingly on t relevance of research for field and landscape scales, and the benefit of their work judged on the welfare of the environment and society. The statistical analytical to presented in this chapter combined with integrative indices of soil quality allow direct on-site analysis and can be considered as one of several important steps updating our landscape–ecological research strategies to achieve sustainable cr production and maintain optimum ecosystem health.

ACKNOWLEDGEMENTS

The authors gratefully acknowledge the most helpful comments of Donald Nielsen and linguistic support by Laura Kindsvater.

REFERENCES

Alemi, M.H., Shahriari, M.R. and Nielsen, D.R. 1988. Kriging and cokriging of soil wa properties. Soil Tech. 1: 117–132.

Assouline, S. 1993. Estimation of lake hydrologic budget terms using simultaneous solutior water, heat, and salt balances and a Kalman filtering approach: application to L: Kinneret. Water Resour. Res. 29: 3041–3048.

Bazza, M., Shumway, R.H. and Nielsen, D.R. 1988. Two-dimensional spectral analyses of surface temperature. Hilgardia 56: 1–28.

Bouten, W., Heimovaara, T.J. and Tiktak, A. 1992. Spatial patterns of throughfall and water dynamics in a Douglas Fir stand. Water Resour. Res. 28: 3227–3233.

Cahn, M.D., Hummel, J.W. and Brouer, B.H. 1994. Spatial analysis of soil fertility for s specific crop management. Soil Sci. Soc. Am. J. 58: 1240–1248.

Davis, J.C. 1986. Statistics and data analysis in geology, 2nd ed. Wiley and Sons, New Yc N.Y., U.S.A.

Deutsch, C.V. and Journel, A.G. 1992. GSLIB. Geostatistical software library and us guide. Oxford Univ. Press, New York, N.Y., U.S.A.

Gelb, A. 1974. Applied optimal estimation. Mass, Inst, of Tech. Press, Cambridge, Ma U.S.A.

Goovaerts, P. and Chiang, C.N. 1993. Temporal persistence of spatial patterns mineralizable nitrogen and selected soil properties. Soil Sci. Soc. Am. J. 57: 372–381.

Halvorson, J.J., Smith, J.L., Bolton, H. and Rossi, R.E. 1995. Evaluating shrub-associa spatial patterns of soil properties in a shrub-steppe using multiple-variable geostatist Soil Sci. Soc. Am. J. 59: 1476–1487.

Hutson, J.L. and Wagenet, R.J. 1989. LEACHM, Leaching Estimation And Chemi: Model. Version 2. Center for Environmental Research, Cornell University, Ithaca, N U.S.A.

Isaaks, E.H. and Srivastava, R.M. 1989. Applied Geostatistics. Oxford Univ. Press, N York, N.Y., U.S.A.

Kachanoski, R.G. and De Jong, E. 1988. Scale dependence and the temporal persistenc spatial patterns of soil water storage. Water Resour. Res. 24: 85–91.

Kachanoski, R.G., Rolston, D.E. and De Jong, E. 1985a. Spatial and spectral relationship soil properties and microtopography. I. Density and thickness of A-horizon. Soil Sci. S Am. J. 49: 804–812.

Kachanoski, R.G., Rolston, D.E. and De Jong, E. 1985b. Spatial variability of a cultivated soil as affected by past and present microtopography. Soil Sci. Soc. Am. J. 49: 1082–1087.

Kalman, R.E. 1960. A new approach to linear filtering and prediction problems. Trans. ASME J. Basic Eng. 8: 35–45.

Katul, G.G., Wendroth, O., Parlange, M.B., Puente, C.E. and Nielsen, D.R. 1993. Estimation of in situ hydraulic conductivity function from nonlinear filtering theory. Water Resour. Res. 29: 1063–1070.

Kite, G. 1989. Use of time series analysis to detect climatic change. J. Hydro. 111: 259–279.

Kool, J.B. and Parker, J.C. 1987. Estimating soil hydraulic properties from transient flow experiments: SFIT user's guide. Report of the Electric Power Res. Inst., Palo Alto, Cal., U.S.A.

Morkoc, F., Biggar, J.W., Nielsen, D.R. and Rolston, D.E. 1985a. Analysis of soil water content and temperature using state-space approach. Soil Sci. Soc. Am. J. 49: 798–803.

Morkoc, F., Biggar, J.W., Miller, R.J. and Nielsen, D.R. 1985b. Statistical analysis of sorghum yield: a stochastic approach. Soil Sci. Soc. Am. J. 49: 1342–1348.

Moulin, A.P., Anderson, D.W. and Mellinger, M. 1994. Spatial variability of wheat yield, soil properties and erosion in hummocky terrain. Can. J. Soil Sci. 74: 219–228.

Nielsen, D.R. and Alemi, M.H. 1989. Statistical opportunities for analyzing spatial and temporal heterogeneity of field soils. Plant Soil 115: 285–296.

Nielsen, D.R., Tillotson, P.M. and Vieira, S.R. 1983. Analyzing field-measured soil water properties. Agric. Water Man. 6: 93–109.

Nielsen, D.R., atul, G.G., Wendroth, O., Folegatti, M.V. and Parlange, M.B. 1994a. State-space approaches to estimate soil physical properties from field measurements. Proc. 15th Conf. ISSS, Vol. 2a: 61–85.

Nielsen, D.R., Wendroth, O. and Parlange, M.B. 1994b. Developing site-specific technologies for sustaining agriculture and our environment. Pages 42–47 *in* G. Narayanasamy, ed. Management of land and water resources for sustaining agriculture and our environment. Diamond Jubilee Symposium, Indian Soc. of Soil Sci, New Delhi, India.

Olea, R.A. 1991. Geostatistical glossary and multilingual dictionary. Oxford Univ. Press, New York, N.Y., U.S.A.

Or, D. and Hanks, R.J. 1992. Soil water and crop yield spatial variability induced by irrigation nonuniformity. Soil Sci. Soc. Am. J. 56: 226–233

Parlange, M.B., Katul, G.G., Folegatti, M.V. and Nielsen, D.R. 1993. Evaporation and the field scale soil water diffusivity function. Water Resour. Res. 29: 1279–1286.

Peterson, G.A., Westfall, D.G. and Cole, C.V. 1993. Agroecosystem approach to soil and crop management research. Soil Sci. Soc. Am. J. 57: 1354–1360.

Reichardt, K., Hardarson, G., Zapata, F., Kirda, C. and Danso, S.K.A. 1987. Site variability effect on field measurement of symbiotic nitrogen fixation using the 15N isotope dilution method. Soil Biol. Biochem. 19: 405–409.

Reynolds, W.D., De Jong, R., Vieira, S.R. and Clemente, R.S. 1994. Methodology for predicting agrochemical contamination of groundwater resources. Soil Quality Evaluation Program, Technical Report 4, Centre for Land and Biological Resources Research, Research Branch, Agriculture and Agri-Food Canada, Ottawa, Ont., Canada.

Reynolds, W.D., De Jong, R., van Wesenbeeck, I.J. and Clemente, R.S. 1995. Prediction of pesticide leaching on a watershed basis: methodology and application. Water Qual. Res. J. Canada 30: 365–381.

Salas, J.D., Delleur, J.W., Yevjevich, V. and Lane, W.L. 1988. Applied modeling of hydrologic time series. Water Resources Pub., Littleton, Col., U.S.A.

Shumway, R.H. 1985. Time series in soil science: is there life after kriging? *in* D.R. Nielsen and J. Bouma, eds. Soil spatial variability. Proc. Workshop ISSS/SSSA, Las Vegas, Nev., U.S.A.

Shumway, R.H. 1988. Applied statistical time series analysis. Prentice Hall, Englewood Cliffs, N.J., U.S.A.

Smith, J.L., Halvorson, J.J. and Papendick, R.I. 1993. Using multiple-variable indicator kriging for evaluating soil quality. Soil Sci. Soc. Am. J. 57: 743–749.

Trangmar, B.B., Yost, R.S. and Uehara, G. 1985. Application of geostatistics to spatial studies of soil properties. Adv. Agron. 38: 45–94.

Vieira, S. R., Nielsen, D.R. and Biggar, J.W. 1981. Spatial variability of field-measured infiltration rate. Soil Sci. Soc. Am. J. 45: 1040–1048.

Warrick, A.W. and Gardner, W.R. 1983. Crop yield as affected by spatial variations of soil and irrigation. Water Resour. Res. 19: 181–186.

Warrick, A.W., Myers, D.E. and Nielsen, D.R. 1986. Geostatistical methods applied to soil science. Pages 53–82 *in* A. Klute, ed. Methods of soil analysis. Part 1, 2nd Ed. Agronomy 9. Am. Soc. Agron., Madison, Wisc., U.S.A.

Wendroth, O., Al-Omran, A.M., Kirda, C., Reichardt, K. and Nielsen, D.R. 1992. State-space approach to spatial variability of crop yield. Soil Sci. Soc. Am. J. 56: 801–807.

Wendroth, O., Katul, G.G., Parlange, M.B., Puente, C.E. and Nielsen, D.R. 1993. A nonlinear filtering approach for determining hydraulic conductivity functions. Soil Sci. 156: 293–301.

Zhang, R., Rahman, S., Vance, G.F. and Munn, L.C. 1995. Geostatistical analyses of trace elements in soils and plants. Soil Sci. 159: 383–390.

AN EMERGING TECHNOLOGY FOR SCALING FIELD SOIL WATER BEHAVIOR

Donald R. Nielsen, Jan W. Hopmans and Klaus Reichardt

INTRODUCTION

In 1955, Miller and Miller created a new avenue for research in soil hydrology when they presented their pioneering concepts for scaling capillary flow phenomena. Their description of self-similar microscopic soil particle structure and its implications for the retention and transport of soil water stimulated many studies to test how well laboratory-measured soil water retention curves could be coalesced into a single scale mean function (e.g. Klute and Wilkinson 1958). Because the results of ensuing tests were not particularly encouraging except for soils composed of graded sands, their scaling concepts lay idle for several years. At that time, owing to the fact that the pressure outflow (Gardner 1956) and other transient methods for estimating the value of the hydraulic conductivity in the laboratory were at their infancy, few attempts to scale the hydraulic conductivity function were made owing to the paucity of its quantitative observation. And, it was also during that same period that the classical works of Philip (1955, 1957) describing a solution of the Richards' equation shifted attention to infiltration. With field measurements of soil water properties only beginning to emerge (e.g. Richards, Gardner, and Ogata 1956), little information was available relative to the reliability of their measurement or to the variation of their magnitudes to be expected within a particular field or soil mapping unit.

During the 1960s, the development and accepted use of the portable neutron meter to measure soil water content spurned research on field-measured soil water properties. With its availability combined with the well-known technology of tensiometry, field studies of soil water behavior were accelerated in the 1970s. However, soil physicists were soon faced with a dilemma – how to deal with the naturally occurring variability of field soils (Nielsen, Biggar, and Erh 1973) and concomitantly measure within reliably prescribed fiducial limits, the much needed soil water functions associated with the Darcy-Buckingham equation and that of Richards. Extending the concepts of Miller scaling was thought to be a promising answer. The first purpose of this chapter is to provide a historical and pedagogic summary of efforts to scale field-measured unsaturated soil water regimes. The second purpose is to provide additional incentives to continue the research and development of a reliable field technology for ascertaining soil water functions and parameters based upon scaling concepts. With many different kinds of invasive and non-invasive techniques available today to measure soil water and related soil properties (Hopmans, Hendricks, and Selker 1997), scaling opportunities continue to appear both promising and provoking.

THE PRINCIPLE OF MILLER AND MILLER SCALING

Scale-invariant relationships for water properties of homogeneous soils based upon the microscopic arrangement of their soil particles and the viscous flow of water within their pores was proposed by Miller and Miller (1955a, b). Each soil was

assumed to be characterized by a soil water retention curve $\theta(h)$ where θ is the volumetric soil water content and h the soil water pressure head. Through the law of capillarity, the value of h for a particular θ is related to a function of r^{-1} where r is the effective radius of the largest soil pores remaining filled with water. According to Miller and Miller, two soils or porous media are similar when scale factors exist which will transform the behavior of one of the porous media to that of the other. Figure 5.1 illustrates their concept of self-similar microscopic soil particle structure for two soils. The relative size of each of the geometrically identical particles is defined by the particular value of the microscopic scale length λ_i. This kind of similarity leads to the constant relation $r_1/\lambda_1 = r_2/\lambda_2 = r_3/\lambda_3 = \cdots = r_i/\lambda_i$ and to the formulation of a scaled, invariant soil water pressure head h_* such that

$$\lambda_1 h_1 = \lambda_2 h_2 = \cdots = \lambda_i h_i = \lambda_* h_* \tag{5.1}$$

where h_* is the scale mean pressure head and λ_* the mean scale length. Dividing each scale length by the mean scale length reduces (5.1) to

$$\alpha_1 h_1 = \alpha_2 h_2 = \cdots = \alpha_i h_i = h_* \tag{5.2}$$

where α_i are the scale factors having a mean value of unity. The hydraulic conductivity function $K(\theta)$ which relates the soil-water flux density to the force acting on the soil water is analogously scaled

$$\frac{K_1(\theta)}{\lambda_1^2} = \frac{K_2(\theta)}{\lambda_2^2} = \cdots = \frac{K_i(\theta)}{\lambda_i^2} = \frac{K_*(\theta)}{\lambda_*^2} \tag{5.3}$$

where K_* is the scale mean hydraulic conductivity function. Written in terms of scale factors α_i, (5.3) becomes

$$\frac{K_1(\theta)}{\alpha_1^2} = \frac{K_2(\theta)}{\alpha_2^2} = \cdots = \frac{K_i(\theta)}{\alpha_i^2} = K_*(\theta). \tag{5.4}$$

Note that the scale length λ_i has a physical interpretation and that the porosity of each soil is assumed identical. A constant porosity across "similar" soils is an important assumption made in this approach.

INITIAL ATTEMPTS TO SCALE FIELD-MEASURED SOIL WATER PROPERTIES DURING REDISTRIBUTION

Initial attempts to scale field-measured functions $K(\theta)$ and $\theta(h)$ were based upon the assumption that a field soil is ensemble of mutually similar homogeneous domains. Owing to the fact that the total porosity of a field soil is highly variable even within a given soil mapping unit, Warrick, Mullen, and Nielsen (1977) found it necessary to modify the restrictive, constant porosity microscopic scaling concept of Miller and Miller (1955a, b). By introducing the degree of water saturation s (= $\theta\theta_S^{-1}$) with θ_S becoming a second scaling factor, they provided a more realistic description of field soils by relaxing the constraint of constant porosity. Moreover, they avoided a search for a microscopic physical length by merely deriving values of α that minimized the sum of squares

$$SS = \sum_{r=1}^{N}\sum_{i=1}^{M}(h_* - \alpha_r h_i)^2 \tag{5.5}$$

for N macroscopic locations within a field soil and M observations of h. For example, with this minimization, 840 measurements of (θ, h) [samples taken at 6 soil depths and 20 sites (N = 120) within an agricultural field and analyzed in the laboratory with 7 values of h (M = 7)] shown in Fig. 5.2a as $h(s)$ were coalesced into the single curve

$$h_* = -6020s^{-1}\left[(1-s) - 2.14(1-s^2) + 2.04(1-s^3) - 0.69(1-s^4)\right] \tag{5.6}$$

in Fig. 5.2b Warrick et al. (1977). The 2640 values of (K, θ) stemming from field measurements analyzed by the instantaneous profile method for 6 soil depths and 20 locations shown in Fig. 5.3a were coalesced and described by the regression expression

$$\ln K_* = -23.3 + 75.0s - 103s^2 + 55.7s^3, \tag{5.7}$$

as shown in Fig. 5.3b. Although Warrick et al. (1977) abandoned the microscopic geometrical similarity concept of Miller and Miller (1955a, b) and based their scaling method on the similarity between soil hydraulic functions, they noted that values of α_r required for scaling h in (5.6) were not equal to those for scaling K in (5.7). Here, it should also be noted that the values of $h(\theta)$ scaled in (5.6) were those measured in the laboratory on soil cores removed from the field, and values of $K(\theta)$ scaled in (5.7) relied on the laboratory measured values of $h(\theta)$ to obtain estimates of $W(t)$ based upon tensiometric measurements taken in the field.

During the next decade, several others attempted to scale field-measured hydraulic properties (e.g. Ahuja, Naney, and Nielsen 1984a; Ahuja, Nofziger, Swartzendruber, and Ross 1989b; Hills, Hudson, and Wierenga 1989). Rao, Jessup, Hornsby, Cassel, and Pollans (1983) as well as others found that scale factors that coalesced field-measured functions of $K(\theta)$ differed from those that coalesced field-measured functions of $\theta(h)$.

Encouraged by the results of Warrick et al. (1977) and those being discussed (eventually published by the International Atomic Energy Agency, 1984) with a group soil physicists from 11 countries, Simmons, Nielsen, and Biggar (1979) suggested scaling the redistribution of soil water in the instantaneous profile method (Watson, 1966). They assumed a unit hydraulic gradient at the lower boundary of the soil profile and used a common value of β in

$$K(\theta) = K_o \exp\left[\beta(\theta - \theta_o)\right] \tag{5.8}$$

for all locations within a field. The assumption was based on the knowledge being found that in a given field, the slope β of the ln$K$ versus (θ - θ_o) graph was normally distributed and characterized by a reasonably small coefficient of variation. Hence, for redistribution in the absence of evaporation, the flux density of water at the lower boundary of the soil profile becomes (Libardi, Reichardt, Nielsen, and Biggar 1980)

$$az\frac{d\theta}{dt} = -K_o \exp\left[\beta(\theta - \theta_o)\right] \tag{5.9}$$

with θ_o being the soil water content at the beginning of the redistribution and a being defined by

$$\overline{\theta} = a\theta + b \tag{5.10}$$

where b is a constant and $\overline{\theta}$ the mean soil water content from the soil surface to depth z from field data. Integrating (5.9) yields

$$\theta = \theta_o - \frac{1}{\beta}\ln\left(1 + \frac{\beta K_o t}{az}\right). \tag{5.11}$$

With a common value of β and a common initial value of $\overline{\theta}_o$, observations of θ measured at different locations and depths as a function of time were scaled with

$$\theta = \overline{\theta}_o - \frac{1}{\beta}\ln\left(1 + \frac{\beta K_* \tau}{z_*}\right) \tag{5.12}$$

where z_* is a reference depth, $\tau = \omega^2 z_* t(az)^{-1}$ and ω a scale factor defined by $K_o = \omega^2 K_*$ where K_* is the scale mean of all K_o. Simmons et al. (1979) attempted to use (5.12) to coalesce 608 neutron probe measurements of θ at 128 locations within four small field plots during redistribution for one month following steady state infiltration. With their assumptions, the necessity of installing tensiometers was eliminated, thereby allowing a much greater number of locations and depths to be sampled with only a neutron probe. With this simplified method, it was envisioned that a large number of scaling factors could adequately quantify the spatial variability of K_o and its scale mean within the experimental site containing the four plots. The 608 values of θ during redistribution were reasonably coalesced about the scale mean curve (5.12) only if the value θ_o for each depth was adjusted to that of $\overline{\theta}_o$.

INITIAL ATTEMPTS TO SCALE SOIL WATER PROPERTIES DURING INFILTRATION

Technology to accurately measure water behavior in homogeneous soil columns improved significantly during the second decade after the pioneering concepts of Miller and Miller were published. For example, the gamma attenuation method for measuring soil water content and soil bulk density, minature pressure transducers to quickly and accurately measure soil water pressure, highly permeable porous plates and cups for improved measurement or control of soil water pressure, and more theoretical methods for ascertaining $K(\theta)$ and $D(\theta)$ from laboratory observations all became available in a relatively short period. The improved technology soon led to attempts to scale transient soil water conditions in both the laboratory and the field.

Initial laboratory experiments

Using inspectional analysis (Ruark 1935), Reichardt, Nielsen, and Biggar (1972) extended the microscopic scaling concepts of Miller and Miller (1955a, b) by attempting to scale macroscopic observations of horizontal infiltration in different kinds of initially dry, homogeneous soils. For an arbitrary macroscopic length L, Reichardt et al. used the following scale mean values

$$K_* = \frac{\mu K_r}{\rho g \lambda_r^2} \quad D_* = \frac{\mu D_r}{\sigma \lambda_r} \quad h_* = \frac{\lambda_r \rho g h_r}{\sigma} \quad t_* = \frac{\lambda_r \sigma t_r}{\mu L^2} \tag{5.13}$$

to reduce Richards' equation for horizontal flow in the x-direction to

$$\frac{\partial \Theta}{\partial t} = \frac{\partial}{\partial x_*}\left[D(\Theta) \frac{\partial \Theta}{\partial x_*} \right] \tag{5.14}$$

where $x_* = xL^{-1}$, $\Theta = (\theta - \theta_n)(\theta_o - \theta_n)^{-1}$, θ_n is the initial soil water content, θ_o the soil water content at $x = 0$ for $t > 0$, g the acceleration of gravity and ρ, σ and μ the density, surface tension and viscosity of water, respectively. Reichardt et al. chose definitions (5.13) to achieve a formal resemblance to those for microscopic similarity of Miller and Miller. [Footnote: From (5.13) through (5.22), we retain the original symbolism λ for scaling length or factor.] With the solution of (5.14) being

$$x_* = \phi_*(\Theta) t_*^{1/2}, \tag{5.15}$$

plots of the distance to the wetting front x_f versus the square root of infiltration time for different soils (Fig. 5.4) yielded values of λ_r defined by

$$\lambda_r \lambda_*^{-1} = m_r^2 m_*^{-2} \tag{5.16}$$

where m_r is the slope $x_{f_r} t_r^{-1/2}$. Arbitrarily choosing the value of λ for Fresno soil equal to unity, the distance to the wetting front x_f versus $t^{1/2}$ for eight soils shown in Fig. 5.4a were scaled into the single curve of (5.15) for t_* defined by (5.13) with L = 1. See Fig. 5.4b. The soil water diffusivity functions $D(\theta)$ calculated for each soil given in Fig. 5.5a were successfully scaled (Fig. 5.5b) using the scaled diffusivity function

$$D_* = 6 \cdot 10^{-7} \exp(8\Theta). \tag{5.17}$$

Miller and Bresler (1977) subsequently included the slope m_* for the Fresno soil in (5.17) and made the suggestion that a universal equation

$$D(\theta) = 10^{-3} m^2 \exp(8\Theta) \tag{5.18}$$

may exist. Additional research has not been conducted to confirm or reject their suggestion. It should also be noted that h_* and K_* defined by (5.13) were not able to coalesce independently measured values of $\theta(h)$ and $K(h)$ using the scaling procedures used by Reichardt et al. (1972).

Later, Reichardt, Libardi, and Nielsen (1975) extended their testing of (5.15) for infiltration into twelve temperate- and tropical-zone soils whose λ-values ranged over two orders of magnitude. They showed that K_* derived from (5.13) for all 12 soils could be described by

$$K_*(\Theta) = 2.65 \cdot 10^{-19} \exp\left(-12.23\Theta^2 + 29.06\Theta\right) \tag{5.19}$$

as illustrated in Fig. 5.6. Somewhat later, Youngs and Price (1981) also observed that different cumulative infiltration curves for a variety of porous materials individually packed into laboratory columns could be scaled to coalesce into a unique curve. Similar to the results of Reichardt et al. (1972), the scale factors defined in (5.13) for K differed from those for h as well as those for the sorptivity S.

Initial field experiments

Using regression techniques similar to those utilized by Reichardt et al. (1972) and Swartzendruber and Youngs (1974), Sharma, Gander, and Hunt (1980) attempted to scale the 26 sets of field-measured cumulative infiltration data from a 9.6-ha watershed shown in Fig. 5.7a. Values of S and A for each of the 26 data sets were obtained by regression using the 2-term, truncated version of the cumulative infiltration I into a homogeneous soil (Philip 1957)

$$I = St^{1/2} + At + Bt^{3/2} + \cdots \tag{5.20}$$

where the first term S is the sorptivity and the remaining terms account for the force of gravity. The solid line in Fig. 5.7a is calculated from

$$I = \overline{S}t^{1/2} + \overline{A}t \tag{5.21}$$

where $\overline{S}$ and $\overline{A}$ are the mean values of each of the respective sets of S_r and A_r. The solid line in Fig. 5.7b is the scaled cumulative infiltration

$$I_* = \overline{S}t_*^{1/2} + \overline{A}t_* \tag{5.22}$$

where $I_* = \lambda_r I\lambda_*^{-1}$, $t_* = \lambda_r^3 t\lambda_*^{-3}$, r the site index and λ_* arbitrarily chosen as unity. Scale factors λ_r for each of the r sites were obtained by minimizing the sum of squares

$$SS = \sum_{r=1}^{N}\sum_{i=1}^{M}\left[I_*(t_{*i}) - I_r(t_i)\right]^2 \tag{5.23}$$

for all r locations and i observations within the watershed. As shown in Fig. 5.7b, the 26 sets of cumulative infiltration observations were nicely coalesced into a unique curve with these values of λ_r .They also calculated two additional sets of scale factors. One set was derived from the observations of $I(t_i)$ throughout the watershed using the scaling relation $\overline{S} = S_r\lambda_r^{-1/2}$ with (5.21). Another set was similarly derived using the scaling relation $\overline{A} = A_r\lambda_r^{-2}$. Although each of these sets of scale factors tended to coalesce the original observations I into a single curve, neither curve was as well defined as that given in Fig. 5.7b. The three sets of scale factors differed significantly, but were nevertheless correlated. The frequency of each set of scale factors was log-normally distributed, and each manifested no apparent spatial correlation.

Russo and Bresler (1980a) also followed the suggestion of Reichardt et al. (1972) to scale soil water profiles during infiltration. They assumed that cumulative vertical infiltration into a field soil could be described by (5.20) truncated to only the sorptivity term provided t approached zero. For a Green and Ampt (1911) piston-type wetting profile, the truncated (5.20) becomes

$$x_f\left(\theta_o - \theta_f\right) = St^{1/2} \tag{5.24}$$

where x_f is the distance to the wetting front. Using (5.16) with field-measured values of S from (5.24), they obtained scale factors α_i for each of the 120 sites in the 0.8-ha plot (Russo and Bresler 1981). At soil water contents close to saturation, scale factors for S were normally distributed and highly correlated with those obtained for $h(s)$ using (5.21).

In addition, Russo and Bresler (1980a) used a scaling technique similar to that of Warrick et al. (1977) to scale calculated, not measured, values of $\theta(h)$ and $K(h)$.

They used field-measured values of the saturated hydraulic conductivity K_S, the water entry value of the soil water pressure head h_w [defined as the minimum value of h on the main wetting branch of $\theta(h)$ at which $d\theta/dh$ remains equal to zero], the sorptivity S, the saturated soil water content θ_S and the residual water content θ_r to calculate $\theta(h)$ and $K(h)$ for each of the above 120 data sets. They assumed that the soil hydraulic properties were described by

$$\begin{aligned} \theta(h) &= (\theta_S - \theta_r)\left(h_w h^{-1}\right)^{\beta} + \theta_r && h < h_w \\ &= \theta_S && h \geq h_w \\ K(h) &= K_S\left(h_w h^{-1}\right)^{\eta} && h < h_w \\ &= K_S && h \geq h_w \end{aligned} \tag{5.25}$$

where h_w is the water-entry value of h (Bouwer 1966) and β and η are soil constants (Brooks and Corey 1964) calculated from

$$\eta = -5K_S h_w(\theta_S - \theta_r)\left[\pi S^2(\theta_S, \theta_r)\right]^{-1} + 1.25 \tag{5.26}$$

$$\beta = (\eta - 2)2^{-1}. \tag{5.27}$$

Functions (5.25) expressed in terms of degree of water saturation s at each location r were scaled according to

$$h_r(s) = h_*(s)\alpha_r^{-1} \tag{5.28}$$

$$K_r(s) = K_*(s)\alpha_r^2 \tag{5.29}$$

using a minimization procedure similar to that of Warrick et al. (1977) where the field scale means of $h(s)$ and $K(s)$ for N locations are defined as

$$h_*(s) = N^{-1}\left\{\sum_{r=1}^{N}\left[h_r^{-1}(s)\right]\right\}^{-1} \tag{5.30}$$

$$K_*(s) = N^{-2}\left\{\sum_{r=1}^{N}\left[K_r(s)\right]^{1/2}\right\}^{2} \tag{5.31}$$

subject to the condition that

$$N^{-1}\sum_{r=1}^{N}\alpha_r = 1. \tag{5.32}$$

Here, their results were similar to those of Warrick et al. inasmuch as values of α_r for $h(s)$ were correlated but not necessarily equal to those for $K(s)$. Nevertheless, they optimistically concluded that the use of a single scaling factor α as a representative of the soil hydraulic properties of a field remained a practical possibility provided that the water content was expressed as degree of water saturation s.

FUNCTIONAL NORMALIZATION – AN EMPIRICAL ATTEMPT TO SCALE SOIL WATER REGIMES

Tillotson and Nielsen (1984) describing some of the different kinds of scaling techniques used in the physical sciences and engineering, attempted to clarify the

differences between the similar media concept of Miller and Miller and other scaling approaches. Reviewing dimensional methods and noting that no universal nomenclature exists in the literature for distinguishing each of them, they grouped all of the methods into two categories (dimensional analysis and inspectional analysis), provided simple examples of each and introduced the term functional normalization, a regression procedure by which scale factors for soil processes are determined from sets of experimental observations.

The scaling of groundwater levels in relation to the rate of water draining from sandy soil profiles P measured at the outlet of a watershed is an example of functional normalization (Hopmans 1988). The depth to the groundwater z_w within the watershed is influenced by topography, spacing between drainage channels and field soil water properties. Ernst and Feddes (1979) had previously derived the empirical relation

$$P = \chi \exp(-\varepsilon z_w) \tag{5.33}$$

where χ and ε are parameters determined from measurements of P and z_w. Because P is measured only at the outlet of the watershed and z_w is measured with observation wells at r locations, the values of χ differ for each location. Assuming that a common value of ε derived from its average value of all locations $\bar{\varepsilon}$ describes (5.33) for each location, (5.33) becomes

$$P_r = \chi_r \exp(-\bar{\varepsilon} z_w). \tag{5.34}$$

Assuming a scale factor α_r exists such that $\chi_* = \alpha_r \chi_r$, the scaled watershed discharge P_* is given by

$$P_* = \chi_* \exp(-\bar{\varepsilon} z_w). \tag{5.35}$$

In Fig. 5.8a the discharge rate measured only at the outlet of the watershed is plotted against groundwater levels measured at 83 locations within the watershed. Equation (5.35) describes the scaled data where χ_* is 8.52 mm d^{-1} and $\bar{\varepsilon}$ is 3.59 m^{-1}. Hence, by functional normalization, Hopmans (1988) found a set of α_r values that coalesced a large amount of data satisfying (5.34) at each location r to be described by (5.35). Although these values of α_r were not directly related to Miller scaling and have no explicit physical meaning, they were potentially useful to express the variability of the water table levels in a single parameter that may be correlated with other parameters, properties or processes operating within the watershed.

ANALYZING INITIAL SCALING ATTEMPTS

With more than a decade of research testing the applicability of the concept of Miller similitude and related extended theories to laboratory and field-measured soil water properties, the absence of a capacious theory provoked controversy regarding the utility of scaling. Criteria for acceptance or rejection of their application to describe field-measured soil water behavior were without foundation. Moreover, the situation was exacerbated by the fact that no paradigms for local and regional scales of homogeneity in pedology and soil classification had yet been developed.

Sposito and Jury (1985) significantly advanced the analysis of scaling concepts and theories for soil water retention and movement. They improved our

understanding of scaling soil water behavior, and interpreted the results of many scaling experiments. At that time, they provided a unified classification scheme for the three most common macroscopic scaling approaches that had been applied to Richards' equation for one spatial dimension. They scaled Richards' equation subject to those initial and boundary conditions for which most scaling experiments had been performed. Namely, that the initial water content throughout the profile $\theta(z, 0) = \theta_n$, and that the boundary condition at the soil surface was either $\theta(0, t) = \theta_o$ or the water flux density described in terms of $K[\theta(h)]$ and $D[\theta(h)]$. They showed that many scaling parameters developed in an inspectional analysis depend not only upon initial and boundary conditions, but also upon whatever special or unique physical hypotheses are assumed. From their examination of inspectional analyses, three macroscopic similitude approaches were identified – Miller similitude, Warrick similitude and Nielsen similitude. Miller similitude, based upon viscous flow and capillary forces, differs from the original Miller and Miller microscopic approach because a scaling parameter for the volumetric soil water content is required and no hypothesis is made regarding the microscopic geometry of the soil pore structure. Warrick similitude derives scaling factors based on (4) and arbitrarily selected expressions for $K(s)$ and $h(s)$. Nielsen similitude is based on a zero-flux density at the soil surface during redistribution, and the assumption that the hydraulic conductivity, the soil water diffusivity and the soil water retention are exponential functions of soil water content.

Jury, Russo, and Sposito (1987) suggested that the description of the spatial variability of any transient water flow problem involving the scaling of both $K(s)$ and $h(s)$ requires the use of at least three stochastic variates – K_S, α as in (5.28) and η defined by $K = h^{-\eta}$. [Footnote: Twenty years earlier, Corey and Corey (1967) successfully scaled Richards' equation solved for the drainage of laboratory columns each packed with different sized sands provided that the hydraulic conductivity was described by $K = h^{-\eta}$.] Sposito and Jury (1990) theoretically showed that scale factors α_h and α_K defined from equations of the form (5.28) and (5.29), respectively, were related to a third parameter ω by

$$\alpha_K = \alpha_h^{\omega} \tag{5.36}$$

Using the theory of Lie groups, Sposito (1990) showed that Richards' equation will be invariant under scaling transformations of the soil hydraulic properties only when K and D are both either exponential or power functions of θ. Earlier, Ahuja, Nofziger, Swartzendruber and Ross (1989b) had proposed an equation similar to (5.36) relating scaling factors for water saturated hydraulic conductivity K_S and soil water pressure head h_f at the wetting front.

Noting the suggestion of Sposito and Jury (1990) that the microscopic length λ could be defined as that of the "effective" pores rather than that depicted in Fig. 5.1, Snyder (1996) introduced the possibility of a porosity scale factor α_p. With α_p, an alternative form of (5.36) becomes

$$\alpha_K = \alpha_h \alpha_p^n \tag{5.37}$$

where n is a constant dependent upon the model used to describe the hydraulic conductivity function. He suggested that the inclusion of α_P would account for various investigators having obtained values of α_h and α_K which were correlated as well as not correlated (Rao et al. 1983). He also suggested that (5.37) could account for the results of Ahuja, Naney, Green, and Nielsen (1984b) and Ahuja et al. (1989a) where the field-measured values of K_S were proportional to the fourth or fifth power of the effective porosity.

RECENT ATTEMPTS TO SCALE SOIL WATER PROPERTIES

The scaling approach of Miller and Miller (1955a, b) and that of others discussed above based on inspectional analysis and functional normalization sought scale factors that simplified problems by expressing them in terms of a small number of reduced variables. New scaling concepts with their potential application to field conditions continue to be developed. For example, Kutílek, Zayani, Haverkamp, Parlange, and Vachaud (1991) theoretically scaled Richards' equation under an invariant boundary flux condition. This type of scaling has application when water is ponded on a soil having a very thin, less permeable crust at its surface – a condition commonly oberved in many field soils. Warrick and Hussen (1993) developed scaled solutions more general than those of Kutílek et al. in that h specified boundary and initial conditions were considered and were invariant with respect to K_S and h_w. Nachabe (1996) developed theoretical relationships for infiltration between macroscopic capillary length, sorptivity and the shape factor – a measure of the nonlinearity of the soil water diffusivity. He showed that predicted infiltration rate is not very sensitive to different values of the shape factor providing the macroscopic capillary length is the same. With shape factors being difficult to ascertain in the field, the macroscopic capillary length serves as a scale factor. These and other ideas await field investigation.

Field approaches to scale soil water properties and processes

Recently, however, at least four different approaches have been used to scale soil water behavior in the field. The first is whereby a vertically heterogeneous or layered soil profile is transformed into a uniform profile using scale factors to stretch or shrink the thickness of each of the nonuniform soil layers. The second approach is that of linear variability scaling in combination with an inverse technique to solve Richards' equation to estimate in situ soil hydraulic properties. The third approach is whereby slopes of the log-log $h(\theta)$ and $K(\theta)$ relations are used as scaling factors. The fourth approach is that of fractal scaling.

Time-invariant hydraulic gradient in layered soils. Virtually every field soil is heterogeneous with depth, and possesses more or less distinct layers or genetic horizons. Hence the distribution of $h(z, t)$ observed in a field will depend upon the choice of depths at which h is measured. This scaling approach (Sisson 1987) begins with an analysis of the redistribution of soil water under a unit hydraulic gradient (Sisson, Ferguson, and van Genuchten 1980) to estimate $K(\theta)$ without the need for calculating hydraulic gradients and water flux densities from differences of noisy

time- and depth-averaged measurements. With a unit hydraulic gradient Richards' equation reduces to

$$\frac{\partial\theta}{\partial t} = -\frac{dK}{d\theta}\frac{\partial\theta}{\partial z}. \tag{5.38}$$

For an initial condition of

$$\theta(z,0) = \theta_n(z), \tag{5.39}$$

the solution of (5.38), known as a Cauchy problem (Lax 1972), is simply

$$\left.\frac{dK}{d\theta}\right|_{\theta_n} = \frac{z}{t} \tag{5.40}$$

where the soil depth z and the time t are those associated with measured values of θ. Assuming that $K(\theta)$ is an exponential or power function of θ, the function differentiated with respect to θ is equated to zt^{-1} and solved explicitly for $\theta(z, t)$. For a given soil depth, the parameters defining $K(\theta)$ are obtained by regression of a plot of θ versus t.

Sisson (1987) extended the above analysis to a time-invariant hydraulic gradient occurring in layered field soils. The layered soil profile is transformed into a uniform profile by scaling soil depth z in relation to θ and h such that mass and energy are conserved. Richards' equation containing the depth-dependent hydraulic properties $h(\theta, z)$ and $K(\theta, z)$ is transformed into a scaled Richards' equation having hydraulic properties $h_*(\theta_*)$ and $K_*(\theta_*)$ which are independent of soil depth for a scaled depth z_*. Such a transformation is achieved by requiring the following relationships:

$$\frac{\partial K(\theta,z)}{\partial K_*(\theta_*)} = 1 \tag{5.41}$$

$$\frac{\partial h(\theta,z)}{\partial h_*(\theta_*)} = \frac{\partial h}{\partial h_*} \tag{5.42}$$

$$\frac{\partial\theta_*}{\partial\theta} = \frac{\partial z}{\partial z_*}. \tag{5.43}$$

Note that (5.41) requires that all $K(\theta, z)$ curves are parallel. Shouse, van Genuchten, and Sisson (1991) assumed a linear relationship between the scaled soil water profile and the profile measured in the field

$$\theta_*(z_*,t) = a(z) + b(z)\theta(z,t) \tag{5.44}$$

where the two scale factors a and b depend upon z. Using (5.44) in (5.42) and (5.43), assuming a unit hydraulic gradient during redistribution and satisfying (5.41) by selecting a reference depth at which the unscaled hydraulic conductivity $K(\theta, z)$ is chosen to equal the scaled hydraulic conductivity $K_*(\theta_*)$, they obtained the scaled gravity-drainage equation

$$\frac{\partial\theta_*}{\partial t} = -\frac{\partial K_*(\theta_*)}{\partial z_*} \tag{5.45}$$

which has a solution

$$\frac{dK_*}{d\theta_*} = \frac{z_*}{t} \tag{5.46}$$

similar to (5.40). Using (5.46) to obtain values of θ_* for each measured value of θ at each soil depth, scale factors $a(z)$ and $b(z)$were obtained by regression using (5.44).

Shouse, Sisson, Ellsworth, and Jobes (1992a) and Shouse, Sisson, de Rooij, Jobes, and van Genuchten (1992b) demonstrated the applicability of the above scaling method for observations of soil water within a 4-m^2 plot of a layered soil. Observations of soil water content were obtained during a 3-week period of redistribution following an initially 30-day ponded condition. $\theta(h)$ was estimated from measurements made in the laboratory on soil cores (5 cm diameter, 7 cm length). By using (5.40), the original soil water profile distributions to a depth of 120 cm for 11 redistribution times in Fig. 5.9a led to $dK/d\theta$ versus θ for the 5 depths shown in Fig. 5.9b. Shown in Fig. 5.10a are the scaled soil water profiles that coalesce the data from all 5 depths into the unique curve of $dK_*/d\theta_*$ shown in Fig. 5.10b using (5.41). Hence, this approach requires one set of reference functions for $\theta(h)$ and $K(\theta)$ as well as two scale factors for each additional horizon or depth considered. It should be noted that this kind of linear $\theta(z)$ scaling is independent of the form of $K(\theta)$ and that the same scale factors scale both $\theta(h)$ and $K(\theta)$.

Inverse solution of Richards' equation. The second scaling approach combines the linear variability scaling technique introduced by Vogel, Cislerova, and Hopmans (1991) with an inverse solution of Richards' equation to determine soil hydraulic properties. After irrigating a 32-ha agricultural field with 0.3 m of water, they estimated the amount of water draining from the soil based on observations of soil water content measured with a neutron meter at 44 locations during a period of 125 d (Eching, Hopmans, and Wallender 1994). With rainfall equaling estimates of evapotranspiration during that 125-d period, net changes of soil water storage from the soil surface to the 2.1-m soil depth were attributed to drainage only. Hence, Richards' equation was solved assuming a zero flux condition for the soil surface and a known flux condition at the bottom of the 2.1-m profile.

At each location r they assumed that the drainage flux density q_r was described by the exponential function (Belmans, Wesselling, and Feddes 1983)

$$q_r = a_r \exp(-b_r t_r) \tag{5.47}$$

where a_r and b_r are fitting parameters and t_r the drainage time beginning when the soil water storage in the profile was a maximum. They used the linear scaling relations proposed by Vogel et al. (1991) for each location r

$$\begin{aligned} K_r(h_r) &= \alpha_{K_r} K_*(h_*) \\ \theta_r(h_r) &= \theta_{res_r} + \alpha_{\theta_r}\left[\theta_*(h_*) - \theta_{res_*}\right] \\ h_r &= \alpha_{h_r} h_* \end{aligned} \tag{5.48}$$

where θ_{res} is the residual soil water content θ_r as in (5.25), and $K_*(h_*)$ and $\theta_*(h_*)$ are the space invariant scale mean soil hydraulic functions. The distributions of α_K and

α_θ were defined such that each must have an arithmetic mean of unity, and $\alpha_{h_r} = 1$ throughout the profile at any location r.

Derived from (5.48), values of $a_r = \alpha_{K_r} a_*$, $b_r = a_r b_r \alpha_{\theta_r}^{-1} a_*^{-1}$ and $t_r = \alpha_{\theta_r} \alpha_{K_r}^{-1} t_*$ were substituted into (5.47) to obtain the scale mean flux density

$$q_* = a_* \exp(-b_* t_*) \tag{5.49}$$

The cumulative drainage Q_r obtained by integrating (5.47) for each location r

$$Q_r = \frac{a_r}{b_r}\left[1 - \exp(-b_r t_r)\right] \tag{5.50}$$

was also similarly scaled to provide the scale mean cumulative drainage Q_*

$$Q_* = \frac{a_*}{b_*}\left[1 - \exp(-b_* t_*)\right] \tag{5.51}$$

In order to meet the constraints that the arithmetic means $\overline{\alpha}_K$ and $\overline{\alpha}_\theta$ were each unity, each set of scale factors was normalized by dividing the values by their respective arithmetic mean. Using the scale mean values $a_* = \overline{\alpha}_K \overline{a}$ and $b_* = a_* \overline{b}(\overline{\alpha}_\theta \overline{a})^{-1}$ in (5.49) or (5.51) defined the lower boundary condition for which Richards' equation was solved. Note that $\overline{a}$ and $\overline{b}$ are the arithmetic means of a_r and b_r, respectively, in (5.47) for the 44 locations. With the inverse solution yielding scale mean functions $\theta_*(h_*)$ and $K_*(\theta_*)$, the soil hydraulic functions at each of the 44 locations were determined from (5.48).

The cumulative drainage $Q(t)$ measured at each of the 44 locations is shown in Fig. 5.11a and the cumulative drainage $Q_*(t_*)$ scaled using (5.51) is shown in Fig. 5.11b. Obtaining scale factors from the simple exponential equation describing drainage from the lower boundary of the soil profiles, the hydraulic functions were easily estimated with a minimal number of soil data by combining the inverse solution of Richards' equation with the linear variability scaling concept.

One-parameter scale model for $h(\theta)$ and $K(h)$. In the third approach, Ahuja and Williams (1991) started with the one-parameter model for $h(\theta)$ proposed by Gregson, Hector, and McGowan (1987). Assuming that θ_r is zero and h < -50 cm, Gregson et al. used (5.25) in the form

$$\ln\left[-h_r(\theta)\right] = u_r + v_r \ln\theta \tag{5.52}$$

to describe $h(\theta)$ at each location r for a large number of soils representing 41 textural classes from Australia and U.K. They found that the u_r versus v_r linear relation

$$u_r = \delta + \zeta v_r \tag{5.53}$$

derived from these diverse soils coalesced together into one common relation with only a small scatter. In other words, Gregson et al. found that each of the values δ and ζ had essentially the same value for all the soils studied. With Ahuja and Williams (1991) finding similar results for ten different U.S. soils, they were encouraged to develop an approach for scaling $h(\theta)$ that would be applicable across

soil types and textural classes. Substituting (5.53) into (5.52) and rearranging, they obtained

$$\ln\theta = \{\ln[-h_r(\theta)] - \delta\}v_r^{-1} - \zeta. \tag{5.54}$$

Assuming values δ and ζ are constant and independent of location, the only parameter in (5.54) that depends upon location is v_r. Hence v_r serves as a scaling factor, and for a fixed value of θ, the right hand side of (5.54) is the same for all r locations.

Ahuja and Williams extended the above approach to also scale unsaturated hydraulic conductivity $K(h)$ data derived from sets of field measurements for six U.S. soils. Assuming that $h < h_w$, they used (5.25) in the form

$$\ln K_r = U_r + V_r \ln(-h) \tag{5.55}$$

to describe $K(h)$ at each location r. They found that the U_r versus V_r linear relation

$$U_r = \xi + \varsigma V_r \tag{5.56}$$

derived from the six data sets shown in Fig. 5.12 coalesced together into a unique relation with R^2 = 0.94. For the individual soils, only the end points of the derived relations within the experimental data range are shown in the figure. The site U_r and V_r values were obtained by regressing (5.55) to the experimental $K(h)$ data for the respective sites. Substituting (5.56) into (5.55), they obtained

$$\ln(-h) = (\ln K_r - \xi)V_r^{-1} - \varsigma \tag{5.57}$$

and used V_r as a scaling factor for each r location. Using constant values of ξ and ς obtained from data for all soils combined in (5.57), the scaled values were adequately coalesced into a single curve.

Fractal scaling. For the fourth approach, Tyler and Wheatcraft (1990) provided fractal scaling insights into the power-law models of soil water retention (5.25) developed empirically by Brooks and Corey (1964) and Campbell (1974). They considered the porous structure of a soil to be represented by a simple fractal in two dimensions known as the Sierpinski carpet generated by starting with an initial square of side length a and removing one or more subsquares of size ab_1^{-1}. Increasing the values of b where $b = b_i$ to the ith recursive level yields a carpet everywhere filled with holes as shown in Fig. 5.13 but where only two levels of the recursion are indicated. For i = 1, the large square in the center of the carpet having an edge equal to ab_1^{-1} is first removed. For the first recursion, $b_1 = a3^{-1}$. Next for i = 2, eight squares having an edge equal to ab_2^{-1} ($b_2 = a3^{-2}$ is removed. Assuming the open areas represent the cross-sections of capillary tubes, and after an arbitrary, large number of recursions, we have a distribution of pores in a soil having porosity

$$\phi(b) = 1 - b^{D-2} \tag{5.58}$$

The parameter b is inversely related to the smallest pore size and D is the fractal dimension of the soil and is given by

$$D = \frac{log(b_1^2 - l_1)}{log\, b_1} \tag{5.59}$$

where b_1^{-1} represents the size of the largest pore and l_1 represents the number of pores of size b_1^{-1}. The soil water content $\theta(b)$ associated with water held in pores of size b^{-1} or smaller is from (5.58)

$$\theta(b) = b^{D-2}. \tag{5.60}$$

From the capillary rise equation, h is proportional to b, and hence,

$$\theta(b) \alpha\, h^{D-2}. \tag{5.61}$$

Normalizing (61) in terms of θ_S the Brooks and Corey (1964) or Campbell (1974) form of the soil water retention curve (5.25) is obtained

$$s = \left(h h_w^{-1}\right)^{D-2}. \tag{5.62}$$

They demonstrated that soil water retention curves of clay soils would tend to have large values of D while sandy soils would have smaller values of D.

More recently, Pachepsky, Shcherbakov, and Korsunskaya (1995) extended the fractal concepts of Friesen and Mikula (1987), Tyler and Wheatcraft (1990) and Brakensiek, Rawls, Logsdon, and Edwards (1992) to quantify the spatial variability of $\theta(h)$ in field soils. They started with the fractal relationship

$$\frac{d\theta}{dR} = AR^{2-D} \tag{5.63}$$

where the effective radius R is the scale length measure of pores and A is a constant reflecting the geometry of the soil. Pores of radius $r < R$ are filled with water. From (5.63) they derived

$$\theta = \frac{\theta_c}{2} erfc\left[\frac{1}{\sigma\sqrt{2}} \ln\left(\frac{h}{h_*}\right)\right] \tag{5.64}$$

where h_* is the value of h at r_*,

$$ln\, r_* = ln\, \bar{r} + \sigma^2(3-D), \tag{5.65}$$

$$\ln \theta_c = \ln\left(A\bar{r}^{3-D}\right) + \sigma^2(3-D)^2 / 2, \tag{5.66}$$

and $\bar{r}$ and σ^2 are the geometric mean radius and variance of the pore radius distribution, respectively.

Each soil water retention curve measured on 84 samples of a clay loam taken from a 12,000-m^2 field were used to determine the parameters θ_c, h_* and σ in (64). Plots of $ln\, r_*$ versus σ^2 and $\ln \theta_c$ versus σ^2 shown in Fig. 5.14a and 5.14b, respectively, yielded nearly identical values of the fractal dimension D. In Fig. 5.14a the value of D according to (5.65) is equal to 2.86 while in Fig. 5.14b its value according to (5.66) is 2.82. Results obtained from 60 samples of a loam from a 1,500-m^2 field were also encouraging. Hence, assuming that the geometric mean radius and the fractal dimension are constant for the field soil investigated, Pachepsky et al. suggested that the variance of the pore radius distribution σ^2 could be used as a single variable to quantify the spatial variability of a soil water property. They further suggested that when the probability distribution of σ^2 and values of parameters A and $\bar{r}$ are known, the proposed scaling allows the generation of spatially noncorrelated random fields of $\theta(h)$.

THE EFFICACY OF SCALING FIELD SOIL WATER BEHAVIOR

Although a generalized theory for comprehensively scaling the behavior of field soil water regimes does not exist, and remains today at the cradle of its development, scaling has provided an encouraging degree of success for those coping with the heterogeneity of field soils. For examples indicating the progress achieved, see Warrick (1990) as well as a few additional examples indicated below.

With the potential to characterize the spatial variability of field soil water properties captured with one or more scaling factors, several investigators have used scale factors assumed to be spatially independent to simulate hydrologic processes as well as the measurement of soil water properties of fields (e.g. Luxmoore and Sharma 1980; Bresler and Dagan 1983; Dagan and Bresler 1983; and Tseng and Jury 1993). Recognizing that soil water properties should be spatially correlated, Jury et al. (1987) also provided a method for obtaining different scale factors that included their spatial correlation structure, and illustrated its use with the data sets of Nielsen et al. (1973) and Russo and Bresler (1980a, b).

From scaling observations of infiltration, values of the scaling factor have revealed differences in cropping management. After measuring the rate of infiltration at 50 locations in a transect across an agricultural field, Hopmans (1989) scaled the modified Kostiakov equation in a manner similar to (5.22). The scale factors, shown in Fig. 5.15, manifest different average values across the transect. The first portion of the transect was located in a region planted to sorghum while the remainder had been fallow prior to the infiltration observations. The larger mean value $\overline{\alpha}$ for the region planted to sorghum probably reflects crop-root induced differences in soil pore structure or soil water content at the time infiltration was measured.

Rockhold, Rossi, and Hills (1996) successfully used scale factors to conditionally simulate water flow and tritium transport measured at the Las Cruces Trench Site. Soil water retention data from 448 core samples were scaled according to (5.2) into a scale mean curve using the Brooks and Corey model (5.25) to obtain values of α_h. Parameters for soil water retention were used in the Burdine (1953) relative permeability model to estimate $K(\theta)$. Saturated values of the hydraulic conductivity K_{Sl} were measured in the laboratory on the 448 soil cores and saturated values of the hydraulic conductivity K_{Sf} were also measured in the field using a borehole permeameter at nearly 600 locations. The latter two sets of data were scaled according to (5.4). The probability distributions of each of the three scale factors were found to be lognormal. The horizontal variograms of the log-transformed scale factors for soil water retention and field-measured K_S (Fig. 5.16a, b.) show remarkably similar spatial structure to about a 5-m lag. Interestingly, the log-transformed scale factors for K_{Sl} measured in the laboratory on the same cores used for measuring $\theta(h)$ manifest (Fig. 5.16c.) virtually no spatial structure (a spatially random behavior).

Although Rockhold et al. (1996) followed the advice of Jury et al. (1987) to quantify the spatial structure of the soil hydraulic properties of the Las Cruces Trench Site, they found it not necessary to use three stochastic variates to condition

their simulations of water and solute transport. Using a constant value of θ_S, constant values for the slopes of $s(h)$ and $K(s)$, and the same distribution of α-values in (5.2) and (5.4) to condition the hydraulic properties of the field, simulations of water flow adequately agreed with those measured. They were sufficiently encouraged by their results to speculate that simulating unsaturated water flow at field scale would evolve from its present-day stochastic analysis to a deterministic analysis in the future.

EXPECTATIONS

We expect avenues of intellectual curiosity supported or derived from observations in the field and the laboratory to continue to kindle investigations of scaling soil water regimes. Because potential avenues for the development of a comprehensive set of different kinds of scaling theories remain largely unexplored, opportunities to quantitatively ascertain the efficacy of scaling field soil water regimes must await additional inquiry and creativity. Without a unified comprehensive theory, fragmented, theoretical considerations provide inadequate criteria for success.

We do not anticipate abundant progress until a complete set of field-measured soil water properties for several locations within at least one field is simultaneously and directly observed, analyzed and published. To date, in every reference cited or omitted in this chapter, critical field measurements have been lacking. For example, Nielsen et al (1973) and Shouse et al. (1992a, b) estimated field soil water contents from laboratory measurements of $\theta(h)$ on soil cores. Russo and Bresler (1980b) estimated functions $\theta(h)$ and $K(\theta)$ from field observations of sorptivity and other parameters. Ahuja and Williams (1991) and Rockhold et al. (1996) also estimated field values of $\theta(h)$ from measurements on soil cores analyzed in the laboratory. Although Eching et al. (1994) measured $\theta(z, t)$ in the field with a neutron meter, they made no observations of $h(z, t)$. Moreover, they made no independent confirmation that the functional relations assumed for the hydraulic properties in the inverse method were descriptive of the field soil studied. On the other hand, both Eching et al. (1994) and Rockhold et al. (1996) explicitly showed that values of K_S measured in the laboratory on soil cores were different than those measured *in situ*. In Fig. 5.17 laboratory determined values of K_S are an order of magnitude greater than those estimated in the field.

Progress toward improved scaling concepts should be accelerated as investigators take the opportunity to simultaneously study details of both an experiment and a theory (e.g. Flühler, Ardakani, and Stolzy 1976). Present-day scaling attempts are confounded by not recognizing that most experimental observations are subject to space- and time-dependent instrumental responses (Baveye and Sposito 1985). And, more attention should be given to the consequences of selecting simplified theoretical models to analyze and scale field-measured data (Tseng and Jury 1993). Presently, no criteria are established to ascertain appropriate soil-depth or time intervals at which observations should be taken. The choice of horizontal spacings between observations remains *ad hoc*. Functional forms of soil hydraulic properties remain without theoretical foundation. Indeed, a dilemma persists regarding how to include "preferential" flow

near water saturation. If K_S is dominated by "preferential" flow, should the relative hydraulic conductivity function $K(s)K_S^{-1}$ be scaled (Jury et al. 1987; Ahuja and Williams 1991) or should that "preferential" flow be described by equations other than that in Richards' equation (e.g. Germann and Beven 1985) and scaled independently? When and how should laboratory studies complement field investigations? Equipment and methods for ascertaining the essential observations are readily available to those wishing to make a contribution to the development of scaling technology. Paradigms for scaling steady-state, one-directional Buckingham-Darcy flow are anticipated to be less restrictive than those for Richards' equation describing transient flow in one or more directions.

We believe information derived from laboratory investigations at the soil pore scale obtained with computed microtomography, magnetic resonance imaging and other noninvasive techniques will improve the use of fractal concepts by Tyler and Wheatcraft (1990) to describe $\theta(h)$ and by Shepard (1993) to calculate $K(\theta)$. The logical next step based on fractals would extend the descriptions and calculations to a field scale as other fractal properties and processes within field soils become better known and understood (Burrough 1983a, b).

Eventually, appropriate scale factors of field-measured soil water properties and processes will be measured in sufficient quantity and detail to analyze and document their spatial and temporal statistical variance structures across and within the landscape. With their values being linked to other soil properties through state-space and other regionalized variable analyses (e.g. Wendroth, Katul, Parlange, Puente, and Nielsen 1993), we anticipate that new paradigms for local and regional scales of homogeneity in pedology and soil classification will emerge. With soil mapping units embracing magnitudes and distributions of spatial and temporal soil-water scale factors, unlimited opportunities will unfold. We expect the numerous uniquely scaled solutions of Buckingham-Darcy and Richards' equations now only theoretically available (e.g. Kutílek et al. 1991; Warrick and Hussen 1993; Nachabe 1996) to be extended to specific landscape and field regions categorized by mapping units described by information containing scale factors for their soil water properties.

REFERENCES

Ahuja, L.R., Cassel, D.K., Bruce, R.R., and Barnes, B.B. 1989a. Evaluation of spatial distribution of hydraulic conductivity using effective porosity data. Soil Sci. 148: 404-411.

Ahuja, L.R., Naney, J.W., and Nielsen, D. R. 1984a. Scaling to characterize soil water properties and infiltration modeling. Soil Sci. Soc. Am. J. 48: 970-973.

Ahuja, L.R., Naney, J.W., Green, R.E., and Nielsen, D.R. 1984b. Macroporosity to characterize spatial variability of hydraulic conductivity and effects of land management. Soil Sci. Soc. Am. J. 48: 699-702.

Ahuja, L.R., Nofziger, D.L., Swartzendruber, D., and Ross, J.D. 1989b. Relationship between Green and Ampt parameters based on scaling concepts and field-measured hydraulic data. Water Resour. Res. 25: 1766-1770.

Ahuja, L.R., and Williams, R.D. 1991. Scaling water characteristics and hydraulic conductivity based on Gregson-Hector-McGown approach. Soil Sci. Soc. Am. J. 55: 308-319.

Baveye, P., and Sposito, G. 1985. Macroscopic balance equations in soils and aquifers; the case of space- and time-dependent instrumental response. Water Resour. Res. 21: 1116-1120.

Belmans, C., Wesselling, J.G., and Feddes, R.A. 1983. Simulation model of the water balance of cropped soil: SWATRE. J. Hydrol. 63: 271-281.

Bouwer, H. 1966. Rapid field measurement of air entry value and hydraulic conductivity of a soil as significant parameters in flow system analysis. Water Resour. Res. 2: 729-738.

Brakensiek, D.L., Rawls, W.J., Logsdon, S.D., and Edwards, W.M. 1992. Fractal description of macroporosity. Soil Sci. Soc. Am. J. 56: 1721-1723.

Bresler, E., and Dagan, G. 1983. Unsaturated flow in spatially variable fields. 2. Application of water flow models to various fields. Water Resour. Res. 19: 421-428.

Brooks, R.H., and Corey, A.T. 1964. Hydraulic properties of porous media. Hydrology Paper 3, Colorado St. Univ., Fort Collins.

Burdine, N.T. 1953. Relative permeability calculations from size distribution data. Am. Inst. Min. Metal. Pet. Eng. 198: 71-77.

Burrough, P.A. 1983a. Multiscale sources of spatial variation in soil. I. The application of fractal concepts to nested levels of soil variation. J. Soil Sci. 34: 577-597.

Burrough, P.A. 1983b. Multiscale sources of spatial variation in soil. II. A non-Brownian fractal model and its application in soil survey. J. Soil Sci. 34: 599-620.

Campbell, G.S. 1974. A simple method for determining unsaturated hydraulic conductivity from moisture retention data. Soil Sci. 117: 311-314.

Corey, G.L., and Corey, A.T. 1967. Similitude for drainage of soils. J. Irri. Drainage Division, Proc. Am. Soc. Civil Eng. 93: 3-23.

Dagan, G., and Bresler, E. 1983. Unsaturated flow in spatially variable fields. 1. Derivation of models of infiltration and redistribution. Water Resour. Res. 19: 413-420.

Eching, S.O., Hopmans, J.W., and Wallender, W.W. 1994. Estimation of in situ unsaturated soil hydraulic functions from scaled cumlative drainage data. Water Resour. Res. 30: 2387-2394.

Ernst, L.F., and Feddes, R.A. 1979. Invloed van grondwateronttrekking voor beregening en drinkwater op de grondwaterstand. Nota 1116, ICW, Wageningen, The Netherlands.

Flühler, H., Ardakani, M.S., and Stolzy, L.H. 1976. Error propagation in determining hydraulic conductivities from successive water content and pressure head profiles. Soil Sci. Soc. Am. J. 40: 830-836.

Friesen, W.I., and Mikula, R.J. 1987. Fractal dimensions of coal particles. J. Coll. Interface Sci. 120: 263-271.

Gardner, W.R. 1956. Calculation of capillary conductivity from pressure plate outflow data. Soil Sci. Soc. Am. Proc. 20: 317-320.

Germann, P.F., and Beven, K. 1985. Kinematic wave approximation to infiltration into soils with sorbing micropores. Water Resour. Res. 21: 990-996.

Green, W.H., and Ampt, G.A. 1911. Studies on soil physics: I. Flow of air and water trough soils. J. Agric. Sci. 4: 1-24.

Gregson, K., Hector, D.J., and McGowan, M. 1987. A one-parameter model for the soil water characteristic. J. Soil Sci. 38: 483-486.

Hills, R.G., Hudson, D.B., and Wierenga, P.J. 1989. Spatial variability at the Las Cruces Trench Site. In proc. intl workshop on Indirect methods for estimating the hydraulic properties of unsaturated soils, Riverside, CA. October 11-13, ed. M. Th. van Genuchten, F.J. Leij, and L.J. Lund, pp. 529-538. Riverside: University of California.

Hopmans, J.W. 1988. Treatment of spatially variable groundwater level in one-dimensional stochastic unsaturated water flow model. Agric. Water Mgt. 15: 19-36

Hopmans, J.W. 1989. Stochastic description of field-measured infiltration data. Trans. ASAE 32: 1987-1993.

Hopmans, J.W., Hendricks, J.M.H., and Selker, J.S. 1997. Emerging Techniques for vadose zone characterizarion. In Vadose Zone Hydrology: Cutting across Disciplines. ed. J.W. Hopmans and M.B. Parlange. (in press) Oxford University Press.

International Atomic Energy Agency. 1984. Field soil-water properties measured through radiation techniques. IAEA-TEC-DOC-312, International Atomic Energy Agency, Vienna.

Jury, W.A., Russo, D., and Sposito, G. 1987. The spatial variability of water and solute transport properties in unsaturated soil. II. Scaling models of water transport. Hilgardia 55: 33-56.

Klute, A., and Wilkinson, G.E. 1958. Some tests of the similar media concept of capillary flow: I. Reduced capillary conductivity and moisture characteristic data. Soil Sci. Soc. Am. Proc. 22: 278-281.

Kutílek, M., Zayani, K., Haverkamp, R., Parlange, J.-Y., and Vachaud, G. 1991. Scaling of Richards' equation under invariant flux boundary conditions. Water Resour. Res. 27: 2181- 2185.

Lax, P.D. 1972. The formation and decay of shock waves. Am. Math. Monthly 79: 227-241.

Libardi, P.L., Reichardt, K., Nielsen, D.R., and Biggar, J.W. 1980. Simple field methods for estimating soil hydraulic conductivity. Soil Sci. Soc. Am. J. 44: 3-7.

Luxmoore, R.J., and Sharma, M.L. 1980. Runoff responses to soil heterogeneity: Experimental and simulation comparisons for two contrasting watersheds. Water Resour. Res. 16: 675-684.

Miller, E.E., and Miller, R.D. 1955a. Theory of capillary flow: I. Experimental information. Soil Sci. Soc. Am. Proc. 19: 271- 275.

Miller, R.D., and Bresler, E. 1977. A quick method fo estimating soil water diffusivity functions. Sci. Sci. Soc. Am. J. 41: 1020-1022.

Miller, R.D., and Miller, E.E. 1955b. Theory of capillary flow: II. Practical implications. Soil Sci. Soc. Am. Proc. 19: 267-271.

Nachabe, M.H. 1996. Microscopic capillary length, sorpivity, and shape factor in modeling the infiltration rate. Sci. Sci. Soc. Am. J. 60: 957-962.

Nielsen, D.R., Biggar, J.W. and Erh, K.T. 1973. Spatial variability of field measured soil water properties. Hilgardia 42: 215-259.

Pachepsky, Ya.A., Shcherbakov, R.A., and Korsunskaya, L.P. 1995. Scaling of soil water retention using a fractal model. Soil Sci. 159: 99-104.

Philip, J.R. 1955. Numerical solution of equations of the diffusion type with diffusivity concentration-dependent. Trans. Faraday Soc. 51:885-892.

Philip, J.R. 1957. Numerical solution of equations of the diffusion type with diffusivity concentration-dependent II. Australian J. Phys. 10:29-42.

Rao, P.S.C., Jessup, R.E., Hornsby, A.G., Cassel, D.K., and Pollans, W.A. 1983. Scaling soil microhydrologic properties of Lakeland and Konawa soils using similar media concepts. Agric. water Mgt. 6: 681-684.

Reichardt, K., Libardi, P.L., and Nielsen, D.R. 1975. Unsaturated hydraulic conductivity determination by a scaling technique. Soil Sci. 120: 165-168.

Reichardt, K., Nielsen, D.R., and Biggar, J.W. 1972. Scaling of horizontal infiltration into homogeneous soils. Soil Sci. Soc. Am. Proc. 36: 241-245.

Richards, L.A., Gardner, W.R., and Ogata, G. 1956. Physical processes determining water loss from soil. Soil Sci. Soc. Am. Proc. 20: 310-314.

Rockhold, M.L., Rossi, R.E., and Hills, R.G. 1996. Application of similar media scaling and conditional simulation for modeling water flow and tritium transport at the Las Cruces Trench Site. Water Resour. Res. 32: 595-609.

Ruark, A.E. 1935. Inspectional analysis: A method which supplements dimensional analysis. J. Elisha Mitchell Sci. Soc. 51: 127-133.

Russo, D., and Bresler, E. 1980a. Scaling soil hydraulic properties of a heterogeneous field. Soil Sci. Soc. Am. J. 44: 681-684.

Russo, D., and Bresler, E. 1980b. Field determinations of soil hydraulic properties for statistical analyses. Soil Sci. Soc. Am. J. 44: 697-702.

Russo, D., and Bresler, E. 1981. Soil hydraulic properties as stochastic processes: I. An analysis of field spatial variability. Soil Sci. Soc. Am. J. 45: 682-687.

Sharma, M.L., Gander, G.A., and Hunt, C.G. 1980. Spatial variability of infiltration in a watershed. J. Hydrol. 45: 101-122.

Shepard, J.S. 1993. Using a fractal model to calculate the hydraulic conductivity function. Soil Sci. Soc. Am. J. 57: 300-307.

Shouse, P.J., Sisson, J.B., Ellsworth, T.R., and Jobes, J.A. 1992a. Estimating in situ unsaturated hydraulic properties of vertically heterogeneous soils. Soil Sci. Soc. Am. J. 56: 1673-1679.

Shouse, P.J., Sisson, J.B., de Rooij, G., Jobes, J.A., and van Genuchten, M.Th. 1992b. Application of fixed gradient methods for estimating soil hydraulic conductivity. In proc. intl workshop on Indirect methods for estimating the hydraulic properties of unsaturated soils, Riverside, CA. October 11-13, ed. M. Th. van Genuchten, F.J. Leij, and L.J. Lund, pp. 675-684. Riverside: University of California.

Shouse, P.J., van Genuchten, M.Th., and Sisson, J.B. 1991. A gravity-drainage/scaling method for estimating the hydraulic properties of heterogeneous soils. In Hydrological Interactions between Atmosphere, Soils and Vegetation. Publ.

No. 204, ed G. Kienitz, pp.281-291. Wallingford, Oxfordshire, UK: IAHS Press, Inst. of Hydrology.

Simmons, C.S., Nielsen, D.R., and Biggar, J.W. 1979. Scaling of field-measured soil-water properties. I. Methodology. II. Hydraulic conductivity and flux. Hilgardia 47: 74-173.

Sisson, J.B. 1987. Drainage from layered field soils: Fixed gradient models. Water Resour. Res. 23: 2071-2075.

Sisson, J.B., Ferguson, A.H., and van Genuchten, M.Th. 1980. Simple method for predicting drainage from field plots. Soil Sci. Soc. Am. J. 44: 1147-1152.

Sisson, J.B., and van Genuchten, M.Th. 1991. An improved analysis of gravity drainage experiments for estimating the unsaturated soil hydraulic functions. Water Resour. Res. 27: 569-575.

Snyder, V.A. 1996. Statistical hydraulic conmductivity models and scaling of capillary phenomena in porous media. Soil Sci. Soc. Am. J. 60: 771-774.

Sposito, G. 1990. Lie invariance of the Richards equation. In Dynamics of fluids in hierarchical porous media, ed J. Cushman, pp. 327-347. New York: Academic Press.

Sposito, G., and Jury, W.A. 1985. Inspectional analysis in the theory of water flow through unsaturated soil. Soil Sci. Soc. Am. J. 49: 791-798.

Sposito, G., and Jury, W.A. 1990. Miller similitude and generalized scaling analysis. In Scaling in Soil Physics: Principles and Applications, SSSA Spec. Publ. No. 25, ed D. Hillel and D.E. Elrick, pp. 13-22. Madison: Soil Sci. Soc. Am.

Swartzendruber, D., and Youngs, E.G. 1974. A comparison of physically-based infiltration equations. Soil Sci. 117: 165-167.

Tillotson, P.M., and Nielsen, D.R. 1984. Scale factors in soil science. Soil Sci. Soc. Am. J. 48: 953-959

Tseng, P.-H., and Jury, W.A. 1993. Simulation of field measurement of hydraulic conductivity in unsaturated heterogeneous soil. Water Resour. Res. 29: 2087-2099.

Tyler, S.W., and Wheatcraft, S.W. 1990. Fractal processes in soil water retention. Water Resour. Res. 26: 1047-1054.

Vogel, T., Cislerova, M., and Hopmans, J.W. 1991. Porous media with linearly variable hydraulic properties. Water Resour. Res. 27: 2735-2741.

Warrick, A.W. 1990. Application of scaling to the characterization of spatial variability in soils. In Scaling in Soil Physics: Principles and Applications, SSSA Spec. Publ. No. 25, ed D. Hillel and D.E. Elrick, pp. 39-51. Madison: Soil Sci. Soc. Am.

Warrick, A.W., and Hussen, A.A. 1993. Scaling of Richards' equation for infiltration and drainage. Soil Sci. Soc. Am. J. 57: 15-18.

Warrick, A.W., Mullen, G.J., and Nielsen, D.R. 1977. Scaling field properties using a similar media concept. Water Resour. Res. 13: 355-362.

Watson, K.K. 1966. An instantaneous profile method for determining the hydraulic conductivity of unsaturated porous materials. Water Resour. Res. 2: 709-715.

Wendroth, O., Katul, G. G., Parlange, M. B., Puente, C. E., and Nielsen, D. R. 1993. A non-linear filtering approach for determining hydraulic conductivity functions in field soils. Soil Sci. 56: 293-301.

Youngs, E.G., and Price, R.I. 1981. Scaling of infiltration behavior in dissimilar porous materials. Water Resour. Res. 17: 1065-1070.

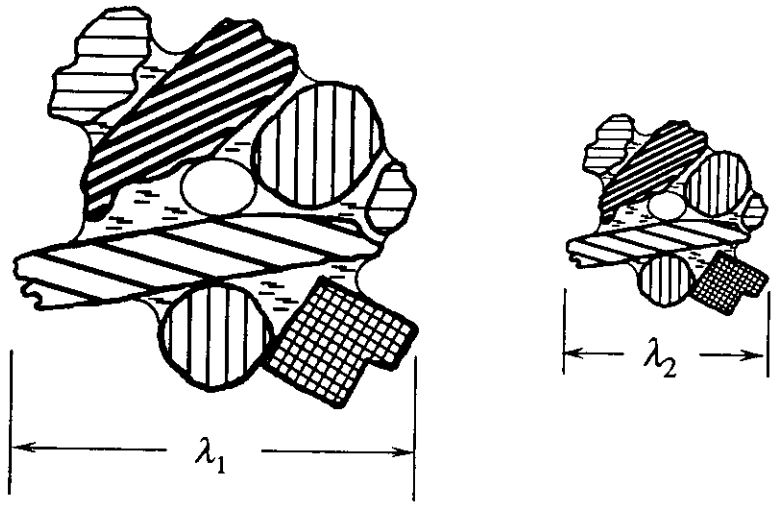

Figure 5.1. A microscopic geometrically similar soil particle arrangement is the principle of Millers' scaling (Miller and Miller, 1955a, b).

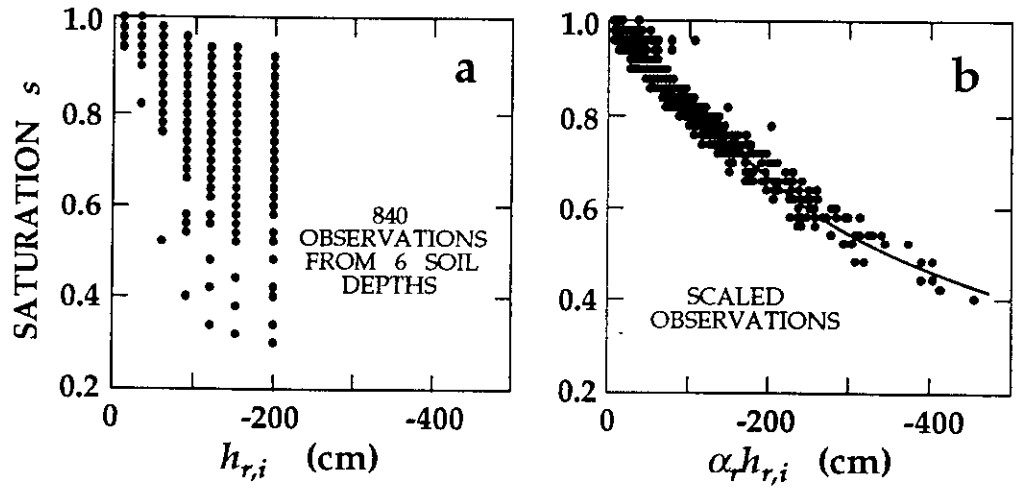

Figure 5.2. a. Unscaled observations of $s(h)$ and b. scaled observations $s(h_*)$ for Panoche soil (Warrick et al., 1977).

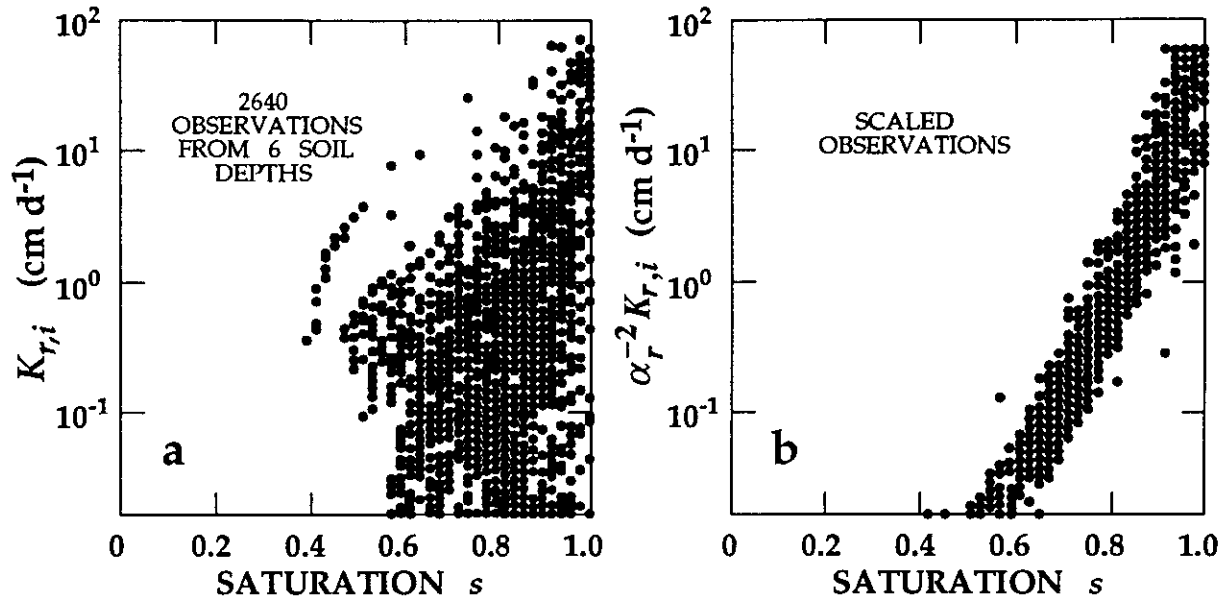

Figure 5.3. a. Unscaled determinations of $K(s)$ and b. scaled determinations $K_*(s)$ for Panoche soil (Warrick et al., 1977).

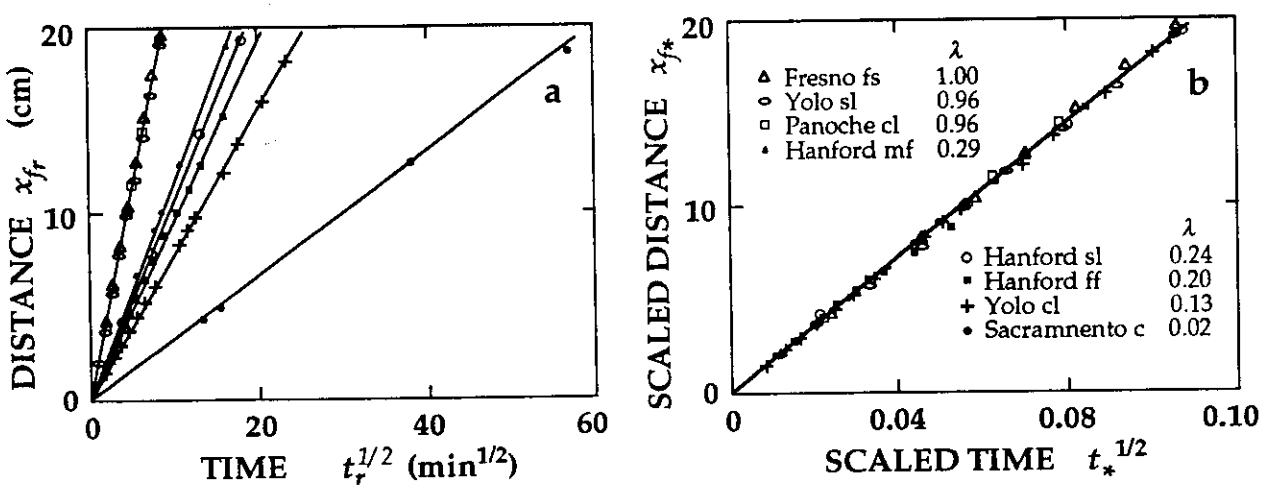

Figure 5.4. a. Unscaled distance to the wetting front x_f, versus $t_r^{-1/2}$ and b. scaled distance x_{f*} versus $t_*^{1/2}$ for horizontal infiltration into 12 air-dry soils (Reichardt et al., 1972).

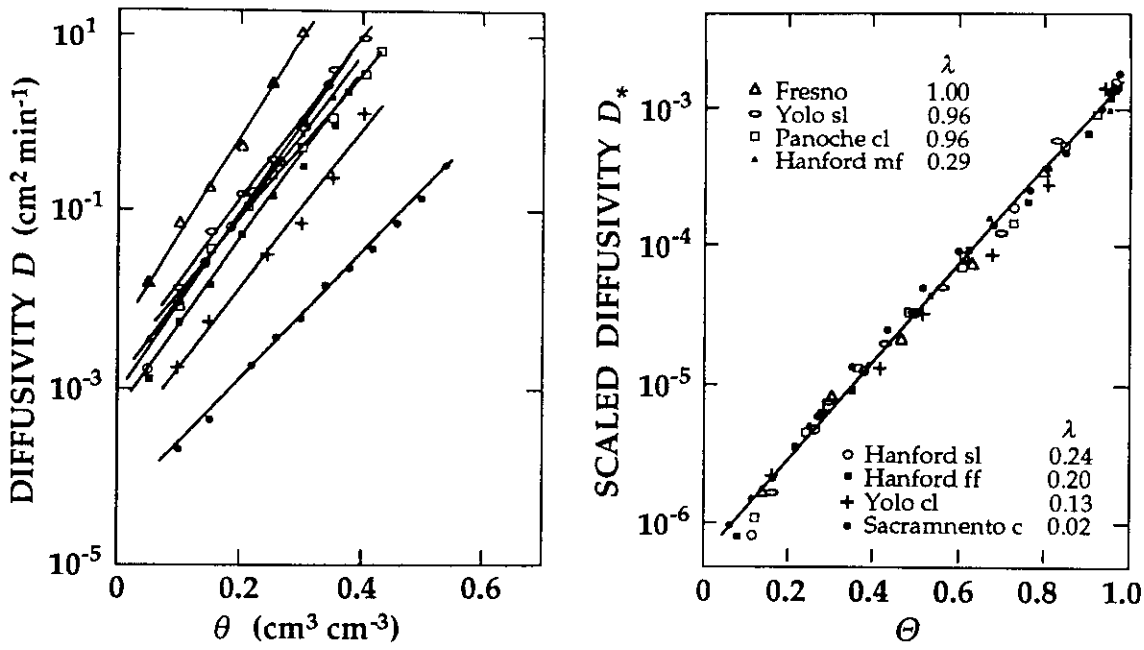

Figure 5.5. a. Unscaled soil water diffusivity $D(\theta)$ and scaled soil water diffusivity $D_*(\Theta)$ for 12 soils (Reichardt et al., 1972).

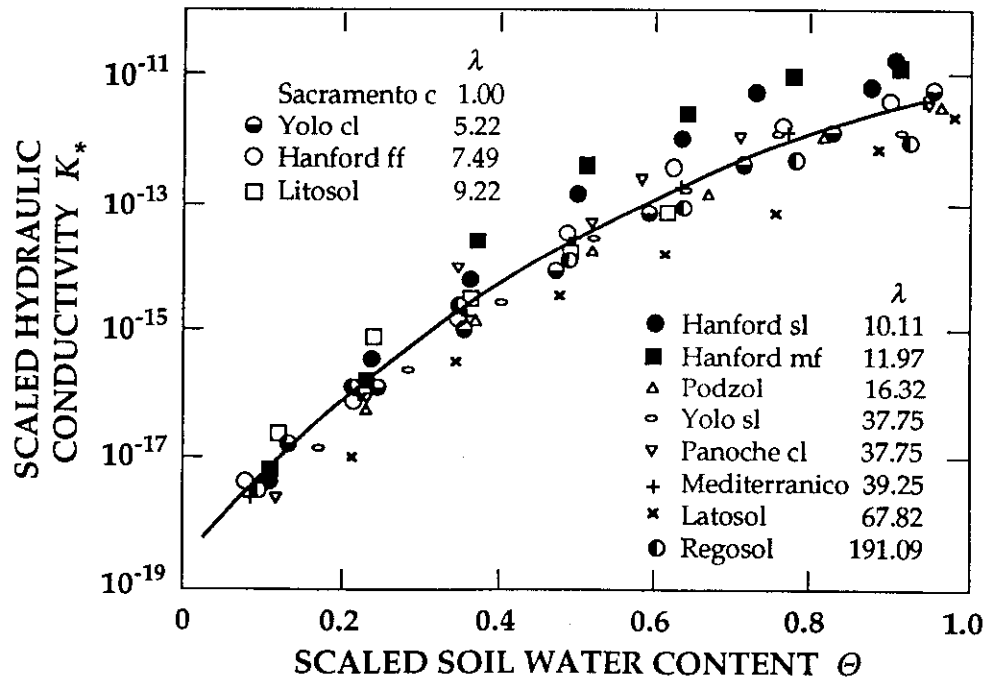

Figure 5.6. Scaled hydraulic conductivity K_* as a function of scaled soil water content Θ (Reichardt et al., 1975).

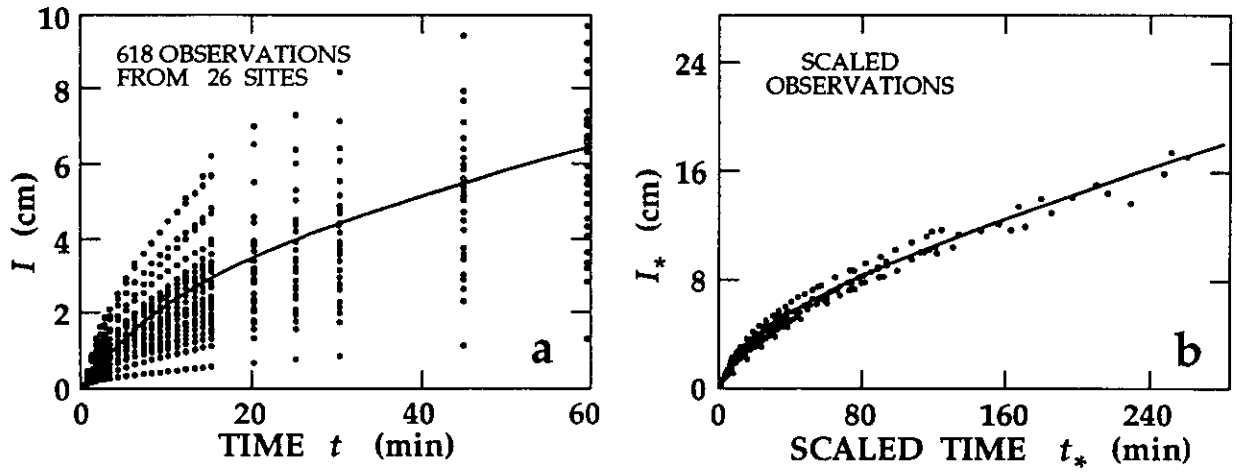

Figure 5.7. a. Unscaled cumulative infiltration versus time and b. scaled cumulative infiltration versus scaled time for 26 sites in a 9.6-ha watershed (Sharma et al., 1980).

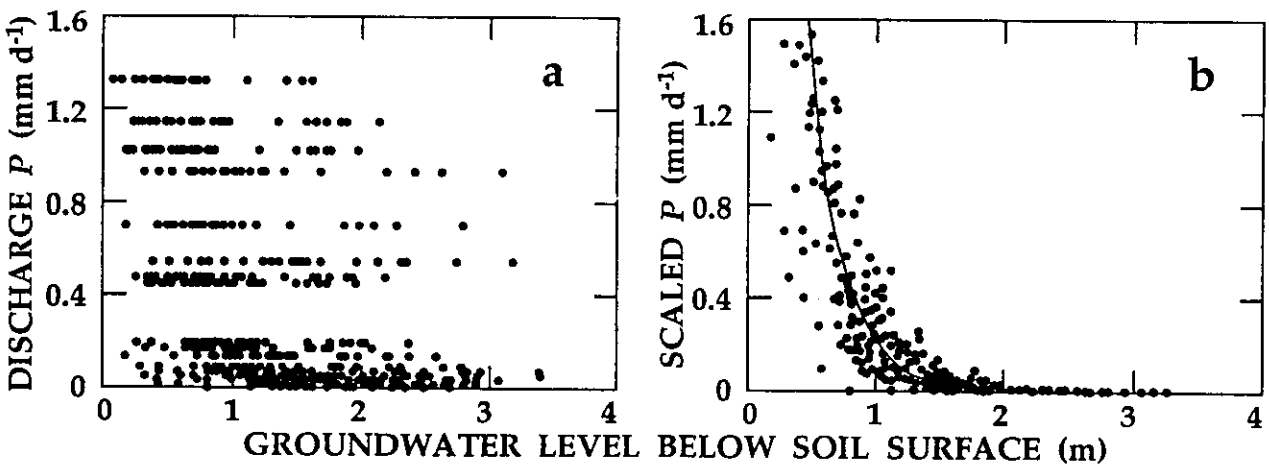

Figure 5.8. a. Unscaled discharge from a watershed as a function of groundwater level below the soil surface. b. Scaled discharge with solid line described by (5.35) (Hopmans, 1988).

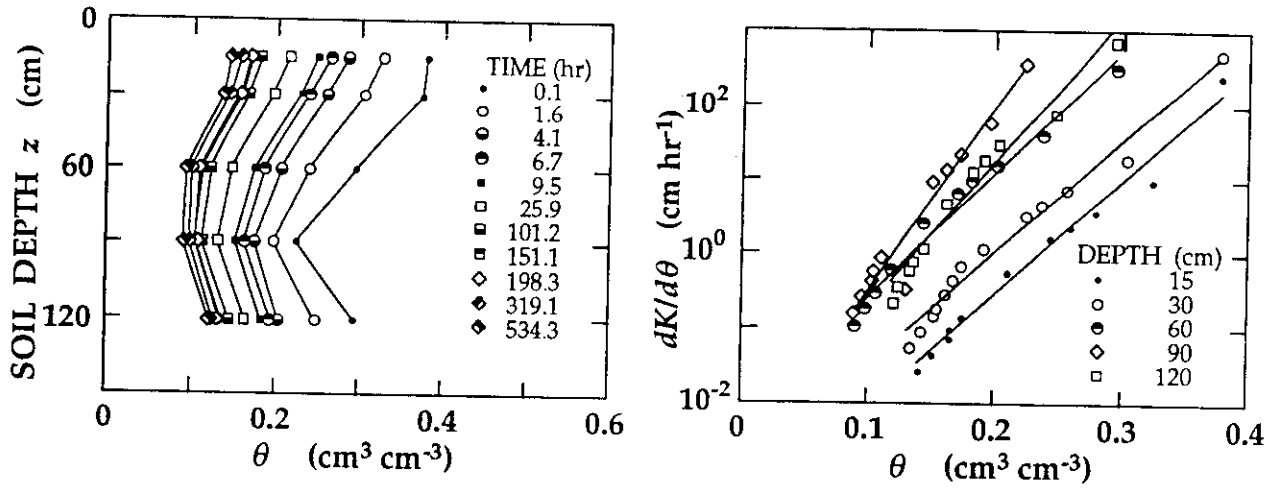

Figure 5.9. a. Measured soil water content profiles for selected times during redistribution and b. calculated values of $dK/d\theta$ versus θ for five soil depths (Shouse et al., 1992).

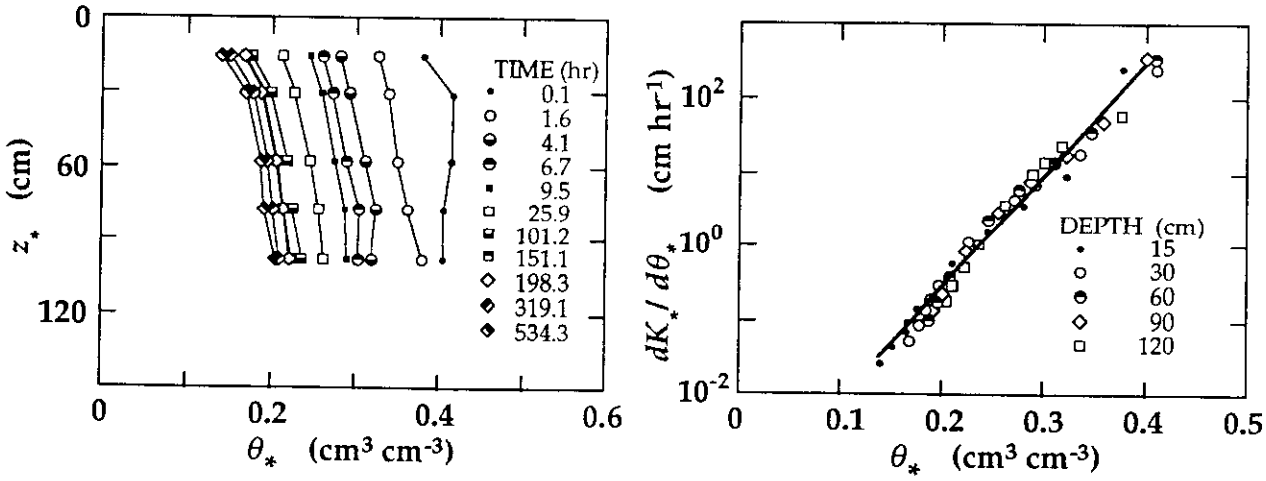

Figure 5.10. a. Scaled soil water content profiles $z_*(\theta_*)$ and b. scaled values $dK_*/d\theta_*$ versus θ_* for the observations given in Figure 5.9 (Shouse et al., 1992).

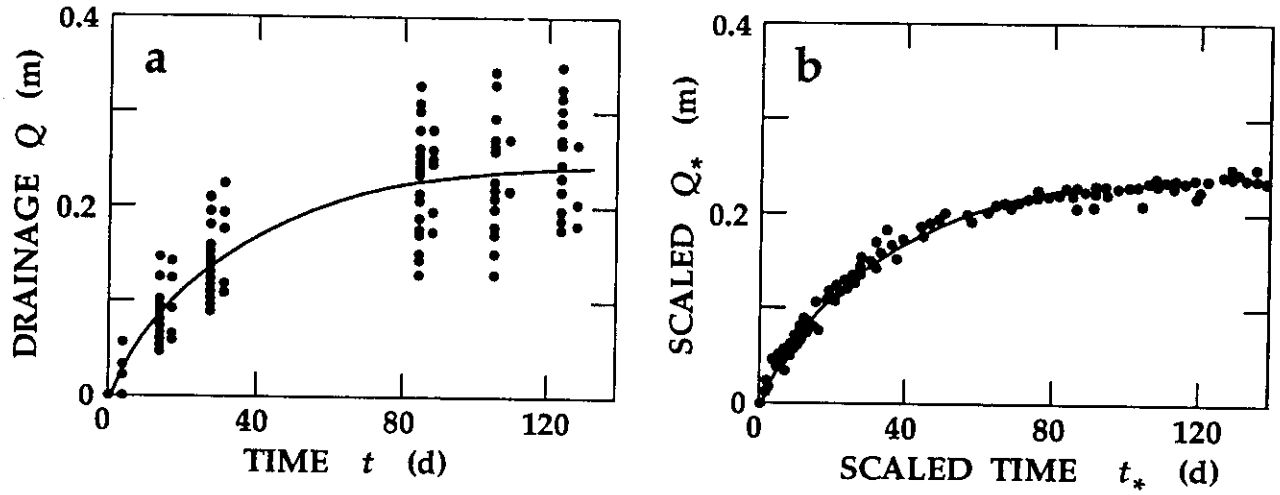

Figure 5.11. a. Unscaled cumlative drainage versus time and b. scaled cumlative drainage at the 2.1-m depth in a 32-ha field (Eching et al., 1994).

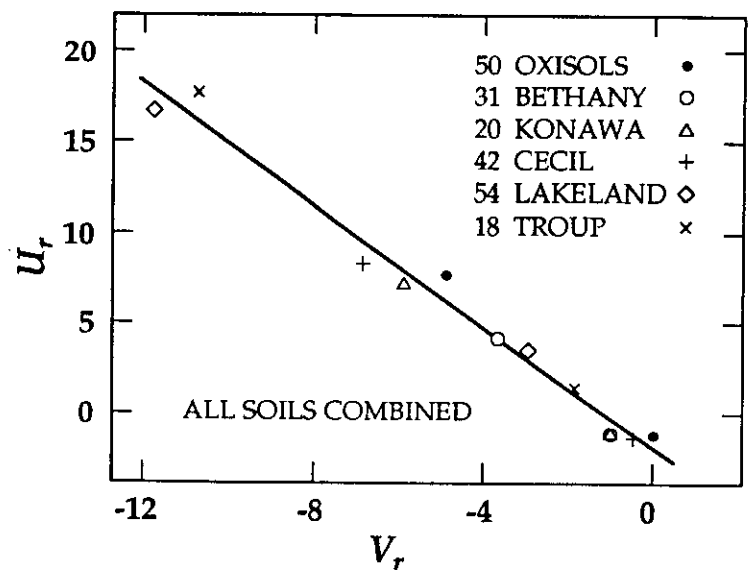

Figure 5.12. The linear U_r and V_r relationships derived by fitting U_r and V_r data for individual sites within each different soil and the site data of all soils combined to (5.56). The units of K and h are cm·hr^{-1} and cm, respectively. The number of sites within each soil are noted next to the soil's name in the figure (Ahuja and Williams, 1991).

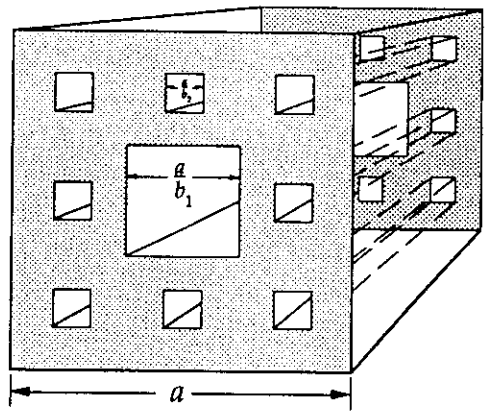

Figure 5.13. Simulated soil using Sierpinski carpet as a conceptual model of pore structure (Tyler and Wheatcraft, 1990).

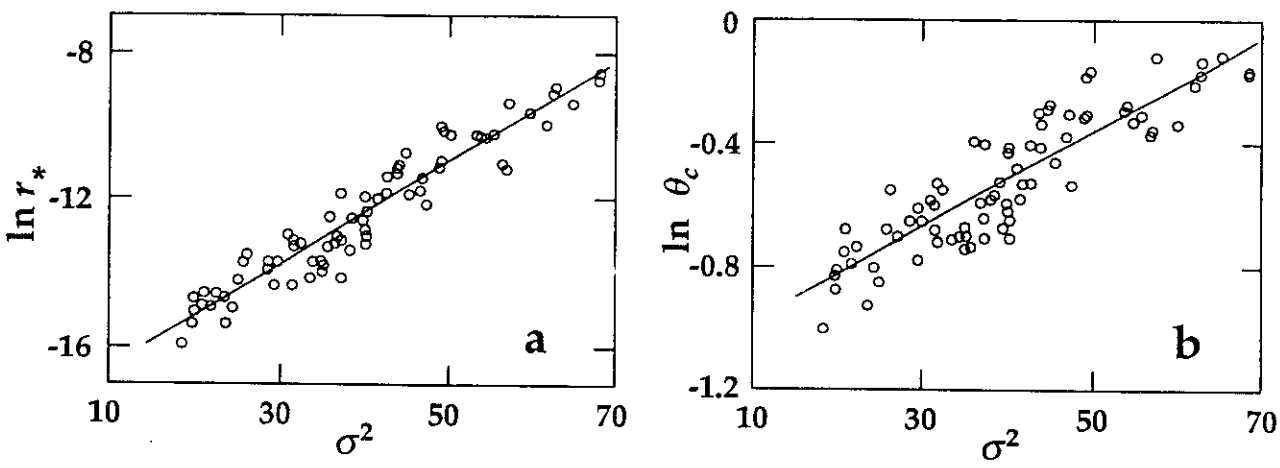

Figure 5.14. a. Linear plot of $\ln r_*$ versus the variance of the pore radius distribution σ^2. b. Linear plot of $\ln\theta_c$ versus the variance of the pore radius distribution σ^2 (Pachepsky et al., 1995).

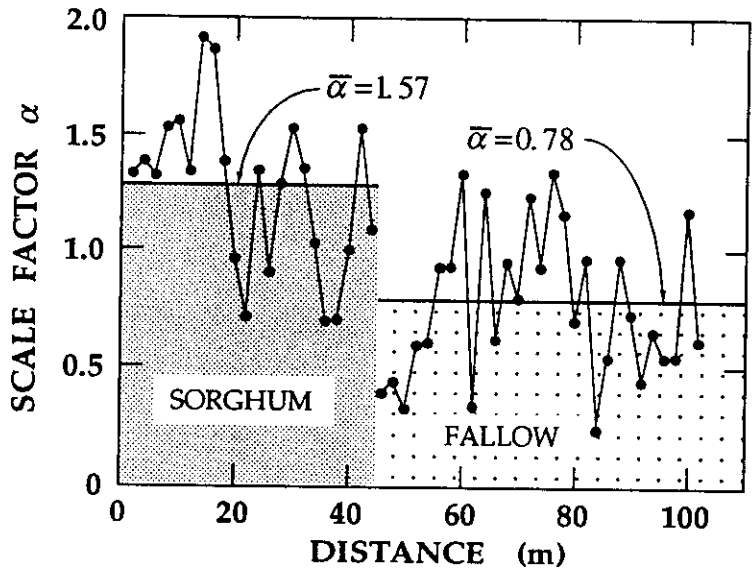

Figure 5.15. Scale factors of infiltration rate measured along a 100-m transect in a partially cropped field (Hopmans, 1989).

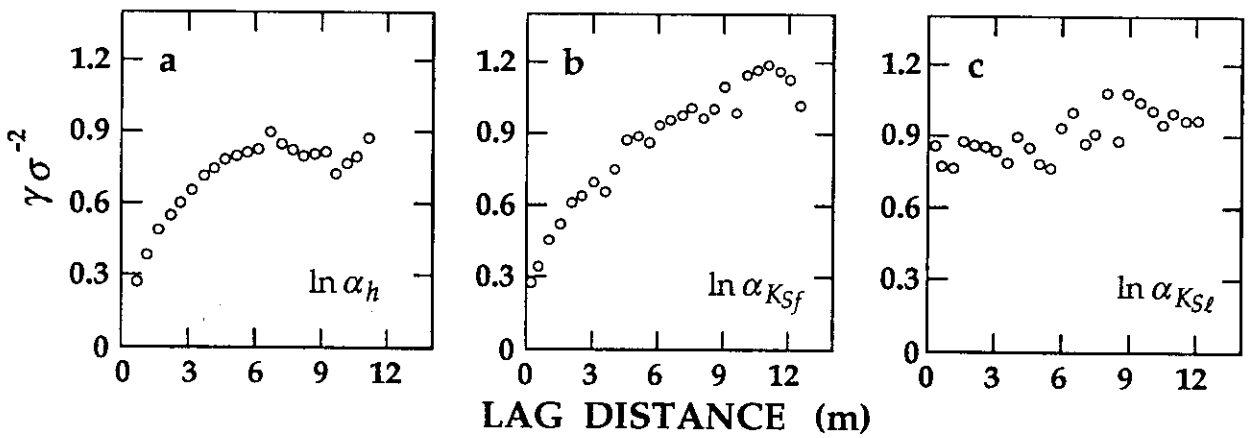

Figure 5.16. a. Normalized horizontal variograms of ln-transformed scaling factors α_h for $\theta(h)$ determined in the laboratory on soil core samples, b. α_{Kf} for field measured saturated hydraulic conductivity and c. α_K for saturated hydraulic conductivity determined in the laboratory on soil core samples (Rockhold et al., 1996).

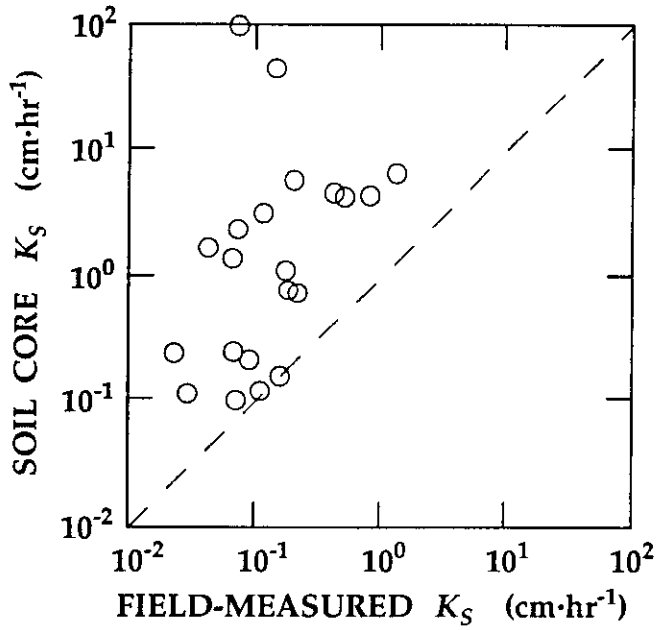

Figure 5.17. Values of water-saturated hydraulic conductivity K_S measured in the laboratory versus those measured in the field (Eching et al., 1994).